A Large Deviation Approach to Spin-Flip Dynamics

Bachelor Thesis
Applied Mathematics and Applied Physics

Written by:
Leo Cazzaniga

Under the supervision of:
Prof.dr. F.H.J. Redig
Prof.dr. S. Stallinga

June 3, 2026
Delft University of Technology
Delft, The Netherlands

Lay Summary

Many processes in nature appear to have a clear direction in time. Heat flows from hot to cold, gases spread out, and ordered systems tend to become disordered. At the microscopic level, however, the rules governing the indiv idual components are often much more symmetric: the reverse evolution is not impossible. This raises a natural question: how can irreversible behavior on a large scale arise from microscopic dynamics that do not clearly prefer one direction of time?

This thesis studies this question using simple models of spins. A spin can be thought of as a small object that can be in one of two states: up or down. When many spins are considered together, their average orientation is called the magnetization. The first model studied in this thesis consists of many spins that flip independently and randomly in time. A single spin behaves unpredictably, but when the number of spins is very large, the average magnetization follows a predictable relaxation towards equilibrium. In this way, deterministic macroscopic behavior emerges from microscopic randomness.

The thesis then studies what happens when the system behaves against this typical relaxation. Such rare fluctuations are possible: the magnetization may temporarily move away from equilibrium instead of towards it. However, these events become extremely unlikely as the number of spins increases. Large deviation theory provides a mathematical framework to estimate how unlikely these rare events are. It also describes the most likely path followed by the system when such an unlikely fluctuation occurs.

Finally, the thesis discusses what changes when spins are no longer independent, but interact with their neighbors. In the Ising model, spins can form large ordered regions, separated by boundaries called interfaces. Rare transitions are then not simply caused by many independent spin flips, but by collective mechanisms such as the formation and growth of a small region of one phase inside another.

The main message of this thesis is that macroscopic irreversibility does not mean that the reverse microscopic evolution is impossible. Rather, in large systems, trajectories opposing relaxation are overwhelmingly unlikely.

Summary

This thesis investigates how irreversible macroscopic relaxation can arise from microscopic spin dynamics, and how rare trajectories opposing this relaxation can be described quantitatively. The main model is an independent spin-flip system of N spins, each taking values in $\{-1, +1\}$ and flipping in time according to an independent Poisson process.

Although the microscopic dynamics are symmetric, the empirical magnetization becomes deterministic in the thermodynamic limit. By the Law of Large Numbers, it converges to $m(t) = e^{-2\lambda t} m(0)$, which describes relaxation towards equilibrium. Fluctuations around this trajectory are of order $N^{-1/2}$ and converge to a Gaussian process, identifiable as an Ornstein–Uhlenbeck process started from zero.

Rare fluctuations beyond this Gaussian regime are studied using large deviation theory. Fixed-time large deviation principles are derived in both quenched and annealed settings, showing that atypical magnetizations are more costly when the microscopic initial configuration is fixed. The analysis is then extended to full trajectories of the magnetization. The pathwise large deviation principle leads to a Hamiltonian and Lagrangian formulation, where rare trajectories are selected as minimizers of an action functional. For prescribed initial and final magnetization, these optimal trajectories are computed explicitly.

Finally, the thesis discusses how this picture changes in interacting systems, using the two-dimensional Ising model as an illustration. Interactions introduce domains, interfaces and metastability, so rare macroscopic irreversibility is no longer produced by independent spin flips, but the geometry of the spins also plays a fundamental role.

The main conclusion is that reversed microscopic trajectories are not impossible. Precisely, trajectories opposing macroscopic relaxation become exponentially unlikely in the system size, and large deviation theory provides a framework to quantify both their probability and their most likely realization.

Contents

Introduction

One of the central questions of statistical physics is how irreversible macroscopic behavior emerges from reversible microscopic dynamics. Although the microscopic dynamics has no preferred direction in time, observables such as entropy, energy, density, or magnetization often relax deterministically towards equilibrium. Understanding how this transition from microscopic reversible randomness to macroscopic irreversible determinism arises is a fundamental problem that bridges between probability theory and statistical mechanics.

In this thesis, we study this phenomenon in the context of a simple stochastic spin-flip model. We consider a system of N independent spins taking values in $\{-1, +1\}$, where each spin flips randomly in time according to an independent Poisson process. Although the microscopic dynamics is entirely stochastic and reversible between the two spin states, the macroscopic magnetization shows a deterministic relaxation towards equilibrium in the limit $N \to \infty$.

The magnetization therefore provides a natural observable through which different probabilistic regimes can be studied. At the macroscopic scale, randomness averages out and the system converges to an irreversible deterministic evolution described by the Law of Large Numbers. At the fluctuation scale, deviations of order $N^{-1/2}$ around the deterministic trajectory are governed by a Central Limit Theorem and converge to a Gaussian process. However, these results only describe typical behavior and Gaussian fluctuations around equilibrium. They do not capture rare trajectories in which the system temporarily evolves against this macroscopic tendency, producing entropy-decreasing fluctuations that become exponentially unlikely as $N \to \infty$. Describing such events requires the framework of large deviation theory.

Large deviations provide asymptotic estimates for exponentially unlikely events and allow us to study not only the probability of atypical fluctuations, but also the associated optimal trajectories. In the pathwise setting, probabilities of atypical trajectories are described through a cost functional, which

resembles the action in classical mechanics. This naturally leads to a Hamiltonian formulation, again in close analogy with classical mechanics. Optimal fluctuation trajectories then arise as minimizers of the corresponding cost functional.

This thesis studies *how the magnetization of a reversible independent spin-flip system exhibits deterministic relaxation in the thermodynamic limit*, and *how rare trajectories opposing this relaxation are quantified by large deviation theory.*

We begin by introducing the independent spin-flip model and studying the macroscopic behavior of the magnetization. The deterministic limit is derived through the Law of Large Numbers. Fluctuations around this limit are then investigated via the Central Limit Theorem.

Next, we study rare events through large deviation theory. We derive fixed-time large deviation principles for the magnetization, distinguishing between the quenched setting, where the initial microscopic configuration is fixed, and the annealed setting, where one additionally averages over the initial fluctuation. The analysis is then extended to trajectories, and the associated pathwise large deviation structure is derived. This leads to a Hamiltonian formulation and to the study of optimal trajectories reaching atypical magnetization values.

Finally, we extend the discussion to interacting systems. In particular, we explore the emergence of irreversible behavior in the two-dimensional Ising model at low temperature. Through numerical simulations, we observe phenomena such as spontaneous symmetry breaking and metastability.

Although the independent spin-flip model is highly simplified, its analytical tractability makes it possible to study the emergence of macroscopic relaxation from microscopic stochastic dynamics in detail. In particular, the model allows explicit characterization of deterministic evolution and fluctuations around equilibrium, as well as the computation of large deviation probabilities of trajectories along which the entropy decreases.

Chapter 1

Macroscopic dynamics and fluctuations

1.1 The independent spin-flip model

We consider N independent spins $\sigma(t) = (\sigma_1(t), ..., \sigma_N(t))$ with values ± 1. Each spin i follows a Poisson clock $N_i(t)$. A Poisson clock with rate λ is a random clock whose ringing times are described by a Poisson process. If $N_i(t) \sim \text{Pois}(\lambda t)$ denotes the number of rings up to time t, then the clock rings on average λt times during a time interval of length t. In our model, each spin flips whenever its clock rings, and different clocks are independent. At time t, we denote the value of each spin by

$$\sigma_i(t) = \sigma_i(0) \cdot (-1)^{N_i(t)}. \tag{1.1}$$

In the following proposition we state and prove some statistical properties of the spins, useful for the coming derivations.

Proposition 1.1. *The probability distribution of each spin value σ_i at time t is given by*

$$\mathbb{P}[\sigma_i(t) = \sigma_i(0)] = \frac{1 + e^{-2\lambda t}}{2}, \qquad \mathbb{P}[\sigma_i(t) = -\sigma_i(0)] = \frac{1 - e^{-2\lambda t}}{2}. \tag{1.2}$$

Furthermore, given the initial configuration $\sigma(0)$, the expected value and variance of each spin $\sigma_i(t)$ at time t are given by

$$\mathbb{E}[\sigma_i(t) \mid \sigma(0)] = \sigma_i(0)\, e^{-2\lambda t}, \tag{1.3}$$

$$\text{Var}[\sigma_i(t) \mid \sigma(0)] = 1 - e^{-4\lambda t}. \tag{1.4}$$

Proof. At time t, $\sigma_i(t) = \sigma_i(0)$ if the spin undergoes an even number of flips, so if $N_i(t)$ is even. Therefore, the probability can be written as

$$\mathbb{P}[\sigma_i(t) = \sigma_i(0)] = \sum_{k=0}^{\infty} \mathbb{P}[N_i(t) = 2k].$$

Since $N_i(t) \sim \text{Pois}(\lambda t)$, we obtain

$$\sum_{k=0}^{\infty} \mathbb{P}[N_i(t) = 2k] = \sum_{k=0}^{\infty} e^{-\lambda t} \frac{(\lambda t)^{2k}}{(2k)!} = e^{-\lambda t} \cosh(\lambda t) = \frac{1 + e^{-2\lambda t}}{2}.$$

For $\sigma_i(t) = -\sigma_i(0)$, we simply take the complementary probability.

Recalling equation (1.1), we know that $\mathbb{E}[\sigma_i(t) \mid \sigma(0)] = \sigma_i(0) \cdot \mathbb{E}[(-1)^{N_i(t)}]$. Using the probability mass function of the Poisson distribution, we get

$$\mathbb{E}[\sigma_i(t) \mid \sigma(0)] = \sigma_i(0) \cdot \sum_{k=0}^{\infty} (-1)^k e^{-\lambda t} \frac{(\lambda t)^k}{k!}.$$

Note that $\sum_{k=0}^{\infty} (-\lambda t)^k / k! = e^{-\lambda t}$ by the power series definition of the exponential. Therefore (1.3) holds.

The variance is calculated as $\mathbb{E}[\sigma_i^2(t) \mid \sigma(0)] - (\mathbb{E}[\sigma_i(t) \mid \sigma(0)])^2$. Using the derived expected value, this becomes $1 - \sigma_i^2(0)\, e^{-4\lambda t}$, where $\sigma_i^2(0) = (\pm 1)^2 = 1$. □

The model is thus described microscopically by the configuration of spins $\sigma(t)$. The microscopic transition is symmetric: each spin flips from $+1$ to -1 and vice versa with the same rate. In this sense the microscopic dynamics does not impose a preferred spin direction, and is therefore reversible. However, irreversibility emerges at the macroscopic scale, as discussed in the coming sections. We first define the magnetization, i.e. the average value of the spins, and determine, as above, its expectation and variance.

Definition 1.1. For the proposed model, we define the magnetization m_N as

$$m_N(t) = \frac{1}{N} \sum_{i=1}^{N} \sigma_i(t). \tag{1.5}$$

Furthermore, define $m(0)$ such that $\lim_{N \to \infty} m_N(0) = m(0)$, assuming the limit exists.

Proposition 1.2. *Given the initial configuration $\sigma(0)$, the expected value and variance of the magnetization m_N at time t are given by*

$$\mathbb{E}[m_N(t) \mid \sigma(0)] = e^{-2\lambda t}\, m_N(0), \tag{1.6}$$

$$\text{Var}[m_N(t) \mid \sigma(0)] = \frac{1}{N}(1 - e^{-4\lambda t}). \tag{1.7}$$

Proof. Using linearity of the expectation, and substituting (1.3) and the definition of $m_N(0)$, we have

$$\mathbb{E}[m_N(t) \mid \sigma(0)] = \frac{1}{N}\sum_{i=1}^{N} \mathbb{E}[\sigma_i(t) \mid \sigma(0)] = \frac{1}{N}\sum_{i=1}^{N} \sigma_i(0)e^{-2\lambda t} = e^{-2\lambda t}\, m_N(0).$$

Similarly, using independence of the spins and additivity of variance for independent random variables:

$$\mathrm{Var}[m_N(t) \mid \sigma(0)] = \frac{1}{N^2}\sum_{i=1}^{N} \mathrm{Var}[\sigma_i(t) \mid \sigma(0)] = \frac{1}{N}(1 - e^{-4\lambda t}).$$

□

Unless stated otherwise, the initial configuration $\sigma(0)$ is regarded as deterministic, and all probabilities and expectations are taken only over the Poisson clocks driving the spin flips. Thus the results below should be read conditionally on the chosen initial configuration.

It is also possible to randomize the initial configuration. In that case, its distribution must be specified separately. A simple choice is to take the initial spins independently, with

$$\mathbb{P}[\sigma_i(0) = +1] = p, \qquad \mathbb{P}[\sigma_i(0) = -1] = 1 - p, \tag{1.8}$$

for some $p \in [0, 1]$. The initial magnetization is then itself a random variable, rather than a fixed number. Later, this distinction between fixing the initial configuration and averaging over random initial data will reappear in the comparison between quenched and annealed descriptions.

1.2 The spin-flip model as a Markov process

The spin-flip dynamics introduced above are an example of a continuous-time Markov process. Before applying this formalism to the model, we briefly recall the main ideas of this theory. The purpose is not to develop the general theory of Markov processes, but to introduce the language of semigroups and generators, which provides a compact way of describing stochastic dynamics and will later be used to derive the large-deviation Hamiltonian.

Let Ω be a finite state space and let $\{X_t, t \geq 0\}$ be a continuous-time stochastic process with values in Ω. The process is called Markovian if, conditionally on the present state, the future evolution is independent of the past. Thus the present state contains all information relevant for the future probabilistic evolution.

In a finite-state Markov jump process, the system remains in a given state for a random time and then jumps to another state. These jumps are described by transition rates. If the process is in state x, the rate $c(x, y)$ gives the instantaneous tendency to jump from x to y, for $x \neq y$. The total rate of leaving the state x is therefore

$$c(x) = \sum_{y \neq x} c(x, y).$$

Rather than describing the process only through the random variable X_t, it is often useful to describe how it acts on observables. An observable is a function $f : \Omega \to \mathbb{R}$. For a Markov process, the associated semigroup S_t is defined by

$$S_t f(x) = \mathbb{E}\left[f(X_t) \mid X_0 = x\right] = \mathbb{E}_x\left[f(X_t)\right],$$

where $\mathbb{E}_x$ denotes expectation in the process starting from $X_0 = x$. Thus $S_t f$ is again a function on the state space: it gives the expected value of the observable f at time t, as a function of the initial state.

The Markov property is reflected in the semigroup identity: $S_{t+s} f = S_t(S_s f) = S_s(S_t f)$ for all $t, s \geq 0$. Indeed, evolving first for time s and then for time t, or vice versa, is probabilistically equivalent to evolving for the total time $t + s$.

The infinitesimal behavior of the semigroup is described by its generator. For a finite-state Markov process, the generator L is defined by

$$Lf = \lim_{t \to 0} \frac{S_t f - f}{t},$$

or, equivalently, pointwise by

$$Lf(x) = \lim_{t \to 0} \frac{\mathbb{E}_x\left[f(X_t)\right] - f(x)}{t}.$$

Hence, Lf represents the instantaneous expected rate of change of the observable f. In particular, the definition gives the small-time expansion

$$S_t f(x) = f(x) + t \cdot Lf(x) + o(t), \qquad \text{as } t \to 0.$$

This formula is often the most useful way to interpret the generator: it describes the first-order change in the expected value of an observable over a very short time interval.

For a jump process with transition rates $c(x, y)$, the generator can be written explicitly as

$$Lf(x) = \sum_{y \neq x} c(x, y)\left[f(y) - f(x)\right]. \tag{1.9}$$

Each term has a direct interpretation. If the process jumps from x to y, the observable f changes by $f(y) - f(x)$, and this possible change is weighted by the rate $c(x, y)$ at which the jump occurs.

Since the state space is finite, the generator can be regarded as a finite-dimensional linear operator acting on functions $f : \Omega \to \mathbb{R}$. In this setting, the semigroup is formally given by the exponential of the generator,

$$S_t = e^{tL}.$$

Equivalently, for each observable f, the function $S_t f$ solves the evolution equation

$$\frac{d}{dt} S_t f = L S_t f = S_t L f.$$

This is the backward equation for the Markov semigroup. It shows that the generator plays the same role for a Markov process as the derivative plays for a deterministic flow: it determines the time evolution infinitesimally.

We now apply this framework to the independent spin-flip model. The state space is

$$\Omega_N = \{-1, +1\}^N.$$

For a configuration $\sigma \in \Omega_N$, let σ^i denote the configuration obtained by flipping the i-th spin:

$$\sigma^i_j = \begin{cases} -\sigma_i, & j = i, \\ \sigma_j, & j \neq i. \end{cases}$$

In the independent spin-flip model, each spin flips at rate λ, independently of all other spins. Therefore, from a configuration σ, the only possible jumps are $\sigma \longrightarrow \sigma^i$ for $i = 1, \ldots, N$, and each such jump occurs with rate λ. Hence the transition rates are $c(\sigma, \sigma^i)$ for $i = 1, \ldots, N$, with no other possible transitions.

It follows from equation (1.9) that, for every observable $f : \Omega_N \to \mathbb{R}$,

$$L_N f(\sigma) = \lambda \sum_{i=1}^{N} \left[f(\sigma^i) - f(\sigma) \right]. \tag{1.10}$$

This is the generator of the microscopic spin process. It encodes the stochastic dynamics in infinitesimal form: for each spin, one computes the change in the observable, i.e. the magnetization, caused by flipping that spin, and then sums these changes with weight λ. In the following chapter, this generator viewpoint will be used to pass from the microscopic dynamics to an effective Markovian description of the magnetization. The generator can already be used to identify the infinitesimal drift of the magnetization.

Proposition 1.3. *Let $m_N(\sigma)$ be the magnetization observable. Then*

$$L_N m_N(\sigma) = -2\lambda m_N(\sigma).$$

Consequently, for the process started from $\sigma(0)$,

$$\mathbb{E}_\sigma \left[m_N \left(\sigma(t) \right) \right] = e^{-2\lambda t} m_N(\sigma(0)).$$

Proof. If the i-th spin is flipped, then only one term in the sum defining the magnetization changes. Hence

$$m_N(\sigma^i) - m_N(\sigma) = \frac{1}{N} \left(-\sigma_i - \sigma_i \right) = -\frac{2\sigma_i}{N}.$$

Applying the generator to the observable m_N, we obtain

$$\begin{aligned} L_N m_N(\sigma) &= \lambda \sum_{i=1}^{N} \left[m_N(\sigma^i) - m_N(\sigma) \right] \\ &= \lambda \sum_{i=1}^{N} \left(-\frac{2\sigma_i}{N} \right) = -2\lambda \frac{1}{N} \sum_{i=1}^{N} \sigma_i = -2\lambda m_N(\sigma). \end{aligned}$$

Using the backward equation for the Markov semigroup, we have

$$\frac{d}{dt} \mathbb{E}_\sigma \left[m_N(\sigma(t)) \right] = \mathbb{E}_\sigma \left[L_N m_N \left(\sigma(t) \right) \right].$$

Substituting the identity just proved gives

$$\frac{d}{dt} \mathbb{E}_\sigma \left[m_N \left(\sigma(t) \right) \right] = -2\lambda \mathbb{E}_\sigma \left[m_N(\sigma(t)) \right].$$

Solving this differential equation, with the initial condition $m_N \left(\sigma(0) \right)$ yields the result above. □

This proposition gives an infinitesimal interpretation of the exponential decay derived earlier from the Poisson-clock representation. At finite N, the magnetization is still a random jump process, not a deterministic differentiable curve. The law of large numbers will show that, in the large-N limit, the random jumps average out and the magnetization itself follows the corresponding deterministic relaxation.

1.3 Boltzmann entropy of the magnetization

The magnetization is a macroscopic observable: it summarizes the state of the system by a single number, but it does not determine the full microscopic configuration. Many different spin configurations may have the same magnetization. This observation is central to the statistical interpretation of irreversibility. Even if the microscopic dynamics do not prefer one sign of the spin over the other, some macroscopic values of the magnetization can be realized by vastly more microscopic configurations than others.

To make this precise, consider the state space $\Omega_N = \{-1, +1\}^N$ and the magnetization $m_N(\sigma)$.

Definition 1.2. For a given value $m \in [-1, 1]$, the Boltzmann entropy associated with the macrostate $m_N(\sigma) = m$ is defined as the logarithm of the number of microscopic configurations realizing this macrostate, normalized by the system size:

$$S_N(m) = \frac{1}{N} \log \# \{\sigma \in \Omega_N : m_N(\sigma) = m\} .$$

Thus $S_N(m)$ measures the number of microscopic realizations of the macroscopic value m on the exponential scale. A macrostate with larger entropy corresponds to a larger number of compatible microscopic configurations.

Proposition 1.4. *The Boltzmann entropy, in the limit $N \to \infty$, is given by*

$$S(m) = -\frac{1+m}{2} \log \left(\frac{1+m}{2} \right) - \frac{1-m}{2} \log \left(\frac{1-m}{2} \right) . \tag{1.11}$$

Proof. Let N_+ and N_- be the number of $+1$ and -1 spins, respectively. Then $N_+ + N_- = N$, while the magnetization is $m = (N_+ - N_-)/N$. Solving these two equations gives

$$N_+ = \frac{N(1+m)}{2}, \qquad N_- = \frac{N(1-m)}{2}.$$

Therefore, fixing the magnetization is equivalent to fixing the number of $+1$ spins. The number of configurations with magnetization m is obtained by choosing which N_+ of the N spins are equal to $+1$. Hence

$$\# \{\sigma \in \Omega_N : m_N(\sigma) = m\} = \binom{N}{N_+} = \binom{N}{\frac{N(1+m)}{2}}.$$

Consequently,

$$S_N(m) = \frac{1}{N} \log \binom{N}{\frac{N(1+m)}{2}}.$$

For large values of N, we use Stirling's approximation. Writing

$$p := \frac{1+m}{2},$$

we compute

$$\begin{aligned}\frac{1}{N} \log \binom{N}{Np} &= \frac{1}{N} \left[\log N! - \log(Np)! - \log(N(1-p))!\right] \\ &= \frac{1}{N} \big[N \log N - N - Np \log(Np) + Np \\ &\qquad - N(1-p) \log(N(1-p)) + N(1-p)\big] + o(1).\end{aligned}$$

The linear terms cancel, and so do the terms with $\log N$. This yields

$$\frac{1}{N} \log \binom{N}{Np} = -p \log p - (1-p) \log(1-p) + o(1).$$

Therefore (1.11) holds. □

The quantity $e^{NS(m)}$ gives the approximate exponential number of configurations with magnetization close to m. Macrostates with larger entropy are therefore overwhelmingly more numerous at the microscopic level. In particular, the entropy is maximal at $m = 0$, where the fractions of positive and negative spins are equal. At this point, $S(0) = \log 2$.

By contrast, at the extreme values $m = 1$ and $m = -1$, all spins must be aligned. Each of these macrostates corresponds to exactly one microscopic configuration, and hence $S(1) = S(-1) = 0$.

This provides the first hint of macroscopic irreversibility. The values $m = \pm 1$ are highly ordered macrostates, realized by very few microscopic configurations. The value $m = 0$, on the other hand, is realized by the largest number of configurations and is therefore overwhelmingly typical. Thus, although the microscopic dynamics are symmetric under the exchange of $+1$ and -1, the macroscopic state $m = 0$ is statistically distinguished by its entropy.

1.4 Deterministic macroscopic evolution

The entropy calculation identifies $m = 0$ as the overwhelmingly typical macrostate, but it does not yet describe the dynamics by which the system

approaches it. To understand the emergence of macroscopic relaxation, we now study the time evolution of the magnetization under the spin-flip dynamics. Through the law of large numbers we show that, although the individual spins evolve randomly, their empirical average becomes deterministic in the limit $N \to \infty$. In the following theorem, the initial configuration $\sigma(0)$ is assumed to be deterministic.

Theorem 1.1. *Assume that the limit $m(0)$ exists such that, as $N \to \infty$, $m_N(0) \to m(0)$. Then, for every fixed $t \geq 0$, as $N \to \infty$,*

$$m_N(t) \to e^{-2\lambda t} m(0) =: m(t).$$

Proof. Let $t \geq 0$ be fixed. We write

$$m_N(t) - e^{-2\lambda t}\, m_N(0) = \frac{1}{N} \sum_{i=1}^{N} \left(\sigma_i(t) - \mathbb{E}\left[\sigma_i(t) \middle| \sigma(0) \right] \right).$$

Conditionally on $\sigma(0)$, the random variables

$$X_i(t) := \sigma_i(t) - \mathbb{E}\left[\sigma_i(t) \mid \sigma(0) \right]$$

are independent, uniformly bounded and have expectation zero. Therefore, by the strong law of large numbers for independent bounded random variables,

$$\frac{1}{N} \sum_{i=1}^{N} X_i(t) \to 0$$

as $N \to \infty$. Hence

$$m_N(t) - e^{-2\lambda t}\, m_N(0) \to 0.$$

Furthermore, by assumption, we know

$$e^{-2\lambda t} m_N(0) \to e^{-2\lambda t} m(0).$$

We can write the following triangle inequality:

$$|m_N(t) - e^{-2\lambda t} m(0)| \leq |m_N(t) - e^{-2\lambda t} m_N(0)| + |e^{-2\lambda t} m_N(0) - e^{-2\lambda t} m(0)|.$$

As $N \to \infty$, since both terms on the right-hand side go to zero, we prove the convergence of $m_N(t)$. □

We have shown that, as the number of spins becomes very large, the randomness of the microscopic flips is no longer visible at the macroscopic level, and the system exhibits a relaxation towards equilibrium. Figure 1.1

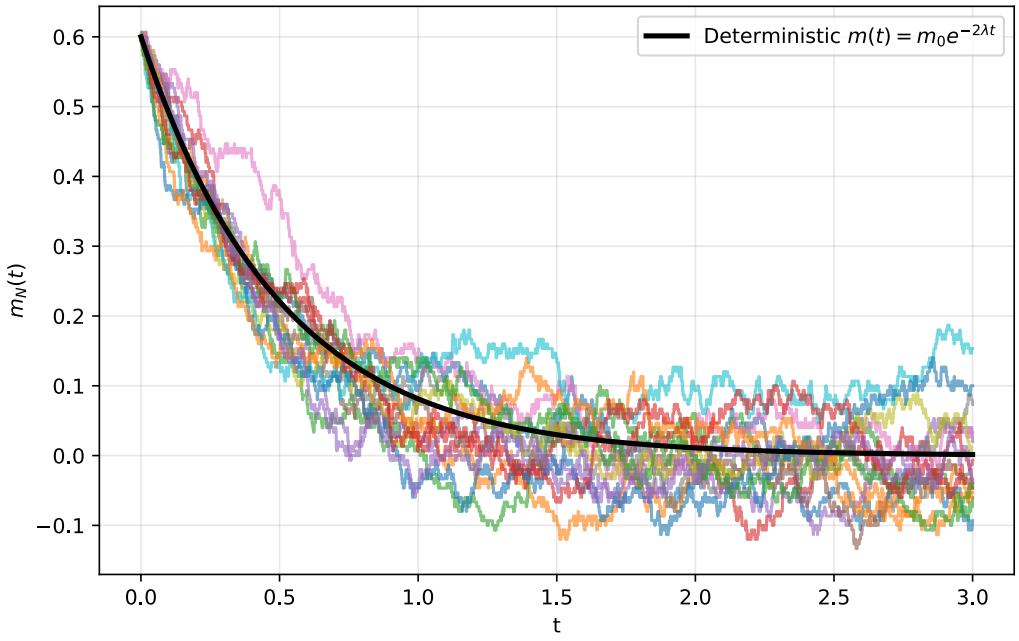

Figure 1.1: Sample trajectories of the magnetization $m_N(t)$ for $N = 300$, obtained from a stochastic simulation of the spin-flip dynamics ($\lambda = 1$), together with the deterministic limit $m(t)$. The trajectories concentrate around the deterministic curve, illustrating Theorem 1.1.

illustrates several simulated trajectories of the magnetization process $m_N(t)$ for finite N, together with the deterministic limit $m(t)$. We observe that, although individual trajectories exhibit stochastic fluctuations, they remain concentrated around the deterministic path, in agreement with the law of large numbers.

Remark 1.1. In the theorem above, the initial configuration is deterministic, and the assumption is that $m_N(0) \to m(0)$ as $N \to \infty$. As anticipated before, one may also choose the initial configuration randomly. If the initial configuration is chosen randomly, then this assumption must be checked.

A sufficient condition is that the initial spins are independent and identically distributed. For example, suppose that $(\sigma_1(0), ..., \sigma_N(0)) \sim \mu^N$, where μ is a probability measure on $\{-1, +1\}$ satisfying

$$\mu(+1) = p, \qquad \mu(-1) = 1 - p.$$

Then the law of large numbers gives

$$m_N(0) = \frac{1}{N} \sum_{i=1}^{N} \sigma_i(0) \to 2p - 1 := m(0).$$

Independence of the initial spins, however, is not necessary. For example, one may choose the initial configuration uniformly among all configurations with a prescribed number N_+ of positive spins. Then the spins are dependent, since fixing the total number of $+1$ spins couples their values. Nevertheless $m_N(0) = (2N_+ - N)/N$ is fixed by construction. If this quantity admits the limit $m(0)$, the same deterministic trajectory holds.

1.5 Fluctuations around equilibrium

The law of large numbers explains the emergence of deterministic macroscopic behavior from reversible microscopic dynamics. However, it also suppresses the randomness that remains for large but finite systems. The variance obtained in equation (1.7) shows that the fluctuations of $m_N(t)$ around its mean are of order $N^{-1/2}$.

To quantify these fluctuations, we study the difference between the magnetization value at time t and the deterministic value. Equivalently, we characterize how far the magnetization is from the deterministic value at time t. This is governed by the central limit theorem. Again, we consider a deterministic initial configuration, assuming that $m(0)$ exists. Note that, in this setting, the spins evolve independently, but are not identically distributed, as two spins i, j with $\sigma_i(0) = +1$ and $\sigma_j(0) = -1$ have different distributions. However, since they are bounded, the central limit theorem still applies.

Theorem 1.2. *Let $t \geq 0$ be fixed. Define the scaled difference between $m_N(t)$ and $e^{-2\lambda t} m_N(0)$ as the random variable*

$$Z_N(t) := \sqrt{N} \left(m_N(t) - e^{-2\lambda t} m_N(0) \right). \tag{1.12}$$

Then, as $N \to \infty$, Z_N converges in distribution to a normal distribution with mean 0 and variance $1 - e^{-4\lambda t}$. In symbols,

$$Z_N(t) \xrightarrow{\mathcal{D}} \mathcal{N}\left(0, 1 - e^{-4\lambda t}\right).$$

Proof. Let $t \geq 0$ be fixed. Conditionally on the initial configuration $\sigma(0)$, define the random variables $Y_i(t)$ and the sum $Z_N(t)$ as follows:

$$\begin{aligned} Y_i(t) &= \sigma_i(t) - e^{-2\lambda t}\, \sigma_i(0), \\ Z_N(t) &= \frac{1}{\sqrt{N}} \sum_{i=1}^{N} Y_i(t). \end{aligned} \tag{1.13}$$

Note that, by substitution, this definition is equivalent to equation (1.12).

Conditionally on $\sigma(0)$, the random variables $Y_i(t)$ are independent. Moreover, recalling the expectation and variance from equations (1.3) and (1.4), we have

$$\mathbb{E}[Y_i(t) \mid \sigma(0)] = \mathbb{E}[\sigma_i(t) \mid \sigma(0)] - e^{-2\lambda t}\sigma_i(0) = 0,$$
$$\mathrm{Var}(Y_i(t) \mid \sigma(0)) = \mathrm{Var}(\sigma_i(t) \mid \sigma(0)) = 1 - e^{-4\lambda t}.$$

Furthermore, the variables $Y_i(t)$ are uniformly bounded:

$$|Y_i(t)| \leq |\sigma_i(t)| + e^{-2\lambda t}|\sigma_i(0)| \leq 2.$$

Let

$$s_N^2 := \sum_{i=1}^{N} \mathrm{Var}(Y_i(t) \mid \sigma(0)) = N(1 - e^{-4\lambda t}).$$

For every $\varepsilon > 0$, the condition $|Y_i(t)| > \varepsilon s_N$ is impossible for all sufficiently large N, because $|Y_i(t)| \leq 2$ while s_N grows like $\sqrt{N}$. Hence Lindeberg's condition[1, p. 137] is satisfied, and by the central limit theorem, as $N \to \infty$,

$$\frac{\sum_{i=1}^{N} Y_i(t)}{s_N} \xrightarrow{\mathcal{D}} \mathcal{N}(0,1).$$

Since $s_N = \sqrt{N(1 - e^{-4\lambda t})}$, this is equivalent to

$$\frac{1}{\sqrt{N}} \sum_{i=1}^{N} Y_i(t) \xrightarrow{\mathcal{D}} \mathcal{N}\left(0, 1 - e^{-4\lambda t}\right).$$

By definition, the left-hand side equals $Z_N(t)$, therefore the theorem holds. □

The fluctuations of the magnetization around its deterministic limit are thus Gaussian, with mean 0 and variance $1 - e^{-4\lambda t}$. This variance increases from 0 at $t = 0$ to 1 in the stationary distribution, i.e. as $t \to \infty$.

To obtain a more complete description of the fluctuations, we extend the analysis from a fixed time t to the full time evolution, i.e. a domain $[0, T]$. We have shown that the deviation from equilibrium at time t is Gaussian. To understand how these deviations evolve, we must keep track of their correlations across time. We therefore consider the rescaled fluctuation process

$$\xi_N(t) = \sqrt{N}\left(m_N(t) - e^{-2\lambda t} m_N(0)\right), \qquad t \in [0, T].$$

In the next theorem, we state that this process converges to a Gaussian process $\xi(t)$. For finite N, the magnetization is piecewise constant: it remains

fixed between flips and changes only when one spin flip occurs. Thus its paths are not continuous, but they are right-continuous and have left limits. Therefore, the convergence of the fluctuation process is understood in the path space $D([0,T])$. This is the space of càdlàg functions, i.e. functions that are right-continuous and have left limits. We equip this space with the Skorokhod topology, which is designed for convergence of paths with jumps: two paths may be close if their jump times differ slightly, provided their values are close after a small deformation of time. As before, the initial configuration of the spins is deterministic.

Theorem 1.3. *For any $T > 0$, as $N \to \infty$, ξ_N converges in distribution to ξ in $D([0,T])$, where ξ is a centered Gaussian process with covariance, for $t, s \in [0,T]$, $t > s$, given by*

$$\mathbb{E}[\xi(t)\xi(s)] = e^{-2\lambda(t-s)} - e^{-2\lambda(t+s)}.$$

Proof. In order to prove convergence in the path space $D([0,T])$, we compute the covariance structure of ξ_N, we apply the multivariate central limit theorem, and we check tightness.

For $t, s \in [0,T]$, $t > s$, using the properties of the Poisson distribution, we compute

$$\mathbb{E}[\sigma_i(t)\sigma_i(s) \mid \sigma(0)] = \mathbb{E}[(-1)^{N_i(t)-N_i(s)}] = e^{-2\lambda(t-s)}.$$

Recalling equation (1.3), this yields

$$\mathrm{Cov}[\sigma_i(t), \sigma_i(s) \mid \sigma(0)] = e^{-2\lambda(t-s)} - e^{-2\lambda(t+s)}.$$

Since the spins are independent, the covariance of ξ_N is unchanged:

$$\mathrm{Cov}[\xi_N(t), \xi_N(s) \mid \sigma(0)] = e^{-2\lambda(t-s)} - e^{-2\lambda(t+s)}.$$

Now fix $0 \leq t_1 < \cdots < t_k$. Then

$$(\xi_N(t_1), \ldots, \xi_N(t_k)) = \frac{1}{\sqrt{N}} \sum_{i=1}^{N} (Y_i(t_1), \ldots, Y_i(t_k)),$$

with Y_i as defined in (1.13), and where the vectors $(Y_i(t_1), \ldots, Y_i(t_k))$ are independent, uniformly bounded and with zero mean. By the multivariate Lindeberg-Feller central limit theorem, as $N \to \infty$, we know that

$$(\xi_N(t_1), \ldots, \xi_N(t_k)) \xrightarrow{\mathcal{D}} \mathcal{N}(0, \Sigma),$$

where Σ is the covariance matrix with entries

$$\Sigma_{a,b} = e^{-2\lambda|t_a - t_b|} - e^{-2\lambda(t_a + t_b)}.$$

It remains to justify tightness in $D([0,T])$. We do not prove this technical step in full, but appeal to the standard functional central limit theorem for independent càdlàg processes [2, ch. 7]. In the present setting the theorem applies because, conditionally on the initial configuration,

$$\begin{aligned}\mathbb{E}\left[(\xi_N(t) - \xi_N(s))^2\right] &= \mathrm{Var}(\xi_N(t)) + \mathrm{Var}(\xi_N(s)) - 2\,\mathrm{Cov}(\xi_N(t), \xi_N(s)) \\ &\le C_T(t-s)\end{aligned}$$

for some constant $C_T > 0$ independent of N.

Finally, we conclude that ξ_N converges to ξ in distribution in the path space $D([0,T])$, where ξ is a centered Gaussian process with the covariance derived above. □

This theorem characterizes the limiting fluctuation process mathematically, but it does not yet give much intuition for how the fluctuations evolve in time.

Remark 1.2. The Gaussian process can be represented as the solution of a stochastic differential equation known as the Ornstein–Uhlenbeck equation:

$$d\xi(t) = -2\lambda\xi(t)\,dt + 2\sqrt{\lambda}\,dB_t,$$

with initial condition $\xi(0)$, and where $B(t)$ is a standard Brownian motion. Its explicit solution is

$$\xi(t) = e^{-2\lambda t}\xi(0) + 2\sqrt{\lambda}\int_0^t e^{-2\lambda(t-u)}\,dB(u).$$

This representation separates the two mechanisms that determine the limiting fluctuations. The first term, $e^{-2\lambda t}\xi(0)$, is the contribution of the initial fluctuation. It is damped exponentially fast by the same relaxation factor that appears in the law of large numbers. Thus, any initial deviation from the deterministic trajectory is gradually forgotten. The integral term represents the fluctuations created by the microscopic spin flips after time 0. The factor $e^{-2\lambda(t-u)}$ shows that a random perturbation produced at time u still affects the system at time t, but its influence decays exponentially with the time difference $t-u$. Recent noise therefore has a stronger effect than noise generated far in the past.

To check that this representation agrees with the covariance obtained in the theorem, assume that $\xi(0) = \xi_0 \sim \mathcal{N}(0, v_0)$. For $0 \leq s \leq t$, substituting in the explicit solution gives

$$\begin{aligned}
\mathbb{E}\left[\xi(t)\xi(s)\right] &= e^{-2\lambda(t+s)} \operatorname{Var}[\xi_0] + 4\lambda \int_0^s e^{-2\lambda(t-u)} e^{-2\lambda(s-u)}\, du \\
&= v_0 e^{-2\lambda(t+s)} + 4\lambda e^{-2\lambda(t+s)} \int_0^s e^{4\lambda u}\, du \\
&= v_0 e^{-2\lambda(t+s)} + e^{-2\lambda(t+s)} \left(e^{4\lambda s} - 1\right) \\
&= e^{-2\lambda(t-s)} + (v_0 - 1) e^{-2\lambda(t+s)}.
\end{aligned}$$

To obtain the same covariance as in the theorem, we must set $v_0 = 0$. This means that ξ_0 is a degenerate Gaussian random variable centered at 0, hence $\xi(0) = 0$. Indeed, as the initial spin configuration at time $t = 0$ is deterministic, there are no fluctuations.

Furthermore, observe that for $v_0 = 1$, we obtain a stationary process. The covariance becomes $e^{-2\lambda(t-s)}$, and taking $t = s$ gives variance 1. This confirms the observation made after the central limit theorem, by taking the limit $t \to \infty$.

1.6 Brief introduction to large deviations

The law of large numbers and the central limit theorem describe the typical behavior of the magnetization. The law of large numbers shows that $m_N(t)$ converges to the deterministic value $m(t)$, while the central limit theorem describes fluctuations of order $N^{-1/2}$ around this value. However, these results do not describe rare events in which the magnetization differs from $m(t)$ by an amount of order one. Such events are much less likely than Gaussian fluctuations, and their probabilities typically decay exponentially fast in the system size N. Large deviation theory provides the framework to quantify this exponential decay [3, 4].

Definition 1.3. Let $(X_N)_{N\geq 1}$ be a sequence of random variables taking values in a topological space E. We say that $(X_N)_{N\geq 1}$ satisfies a large deviation principle with speed N and rate function $I : E \to [0, \infty]$ if I is lower semi-continuous and, for suitable sets $A \subset E$,

$$\mathbb{P}\left[X_N \in A\right] \approx \exp\left(-N \inf_{x\in A} I(x)\right).$$

More precisely, for every closed set $F \subset E$,

$$\limsup_{N\to\infty} \frac{1}{N} \log \mathbb{P}\left[X_N \in F\right] \leq -\inf_{x\in F} I(x),$$

and for every open set $G \subset E$,

$$\liminf_{N\to\infty} \frac{1}{N} \log \mathbb{P}\left[X_N \in G\right] \geq - \inf_{x\in G} I(x).$$

The rate function I measures the exponential cost of observing a given value. Points where $I(x) = 0$ correspond to typical values, while values with $I(x) > 0$ are exponentially unlikely as $N \to \infty$. Informally, we can write

$$\mathbb{P}[X_N \approx x] \asymp e^{-NI(x)}.$$

This notation[1] means that the logarithm of the probability behaves asymptotically as $-NI(x)$.

A standard way to obtain a large deviation principle is through the large deviation free energy, defined as the limiting logarithmic moment generating function. Suppose that the limit

$$\Lambda(\theta) = \lim_{N\to\infty} \frac{1}{N} \log \mathbb{E}\left[e^{N\theta X_N}\right]$$

exists for all $\theta \in \mathbb{R}$. Under suitable regularity assumptions, the Gärtner-Ellis theorem [3, Thm 2.3.6] states that X_N satisfies a large deviation principle with rate function given by the Legendre transform of Λ:

$$I(x) = \sup_{\theta\in\mathbb{R}} \{\theta x - \Lambda(\theta)\}.$$

Thus the free energy plays the role of a generating object from which the exponential cost of rare values can be derived.

In the following section we apply this fixed-time large deviation framework to the magnetization $m_N(t)$.

1.7 Large deviations from the macrodynamics

We first consider the *quenched* setting, which, as in most of the previous results, takes a deterministic initial configuration $\sigma(0)$ and studies only the randomness generated by the spin-flip dynamics. To better understand the role of the initial condition, we also study the *annealed* setting, in which the initial configuration is random, hence the spins at $t = 0$ are identically distributed and independent.

[1] For clarity, the notation $X_N \approx x$ is equivalent to $|X_N - x| < \delta$ for some $\delta > 0$.

1.7.1 Quenched setting

Throughout this subsection, probabilities are understood conditionally on the deterministic initial configuration $\sigma(0)$.

Proposition 1.5. *For fixed $t \geq 0$, in the quenched setting, the large deviation free energy of $m_N(t)$ exists and is given by*

$$\Lambda_t^q(\theta) := \frac{1+m(0)}{2} \log\left(\cosh\theta + e^{-2\lambda t}\sinh\theta\right) + \frac{1-m(0)}{2}\log\left(\cosh\theta - e^{-2\lambda t}\sinh\theta\right),$$

where $m(0)$ is the limit of $m_N(0)$ for $N \to \infty$.

Proof. Recalling the probabilities from (1.2), we compute the moment generating function of $\sigma_i(t)$:

$$\mathbb{E}\left[e^{\theta\sigma_i(t)}\right] = e^{\theta\sigma_i(0)}\frac{1+e^{-2\lambda t}}{2} + e^{-\theta\sigma_i(0)}\frac{1-e^{-2\lambda t}}{2}.$$

Note that, since $\sigma_i(0) = \pm 1$, we have $e^{\pm\theta\sigma_i(0)} = \cosh\theta \pm \sigma_i(0)\sinh\theta$. Then the moment generating function can be written as

$$\mathbb{E}\left[e^{\theta\sigma_i(t)}\right] = \cosh\theta + \sigma_i(0)e^{-2\lambda t}\sinh\theta.$$

We now compute the moment generating function of the magnetization, as defined in (1.5), using the fact that each spin is independent:

$$\begin{aligned}\mathbb{E}\left[e^{N\theta m_N(t)}\right] &= \mathbb{E}\left[e^{N\theta\cdot\frac{1}{N}\sum_{i=1}^N \sigma_i(t)}\right] = \mathbb{E}\left[\prod_{i=1}^N e^{\theta\sigma_i(t)}\right] \\ &= \prod_{i=1}^N \mathbb{E}\left[e^{\theta\sigma_i(t)}\right] = \prod_{i=1}^N \left(\cosh\theta + \sigma_i(0)e^{-2\lambda t}\sinh\theta\right).\end{aligned}$$

Taking the logarithm, we obtain the expression for $\Lambda_{N,t}^q$:

$$\Lambda_{N,t}^q(\theta) = \frac{1}{N}\sum_{i=1}^N \log\left(\cosh\theta + \sigma_i(0)e^{-2\lambda t}\sinh\theta\right).$$

It remains to take the limit $N \to \infty$. Using the indicator functions

$$\mathbf{1}_{\{\sigma_i(0)=1\}} = \frac{1+\sigma_i(0)}{2}, \qquad \mathbf{1}_{\{\sigma_i(0)=-1\}} = \frac{1-\sigma_i(0)}{2},$$

we can split the sum in two terms as follows:

$$\Lambda^q_{N,t}(\theta) = \frac{1}{N}\sum_{i=1}^{N} \frac{1+\sigma_i(0)}{2} \log\left(\cosh\theta + e^{-2\lambda t}\sinh\theta\right) + \frac{1}{N}\sum_{i=1}^{N} \frac{1-\sigma_i(0)}{2} \log\left(\cosh\theta - e^{-2\lambda t}\sinh\theta\right).$$

Since the logarithmic factors do not depend on i, we rewrite,

$$\Lambda^q_{N,t}(\theta) = \frac{1+m_N(0)}{2} \log\left(\cosh\theta + e^{-2\lambda t}\sinh\theta\right) + \frac{1-m_N(0)}{2} \log\left(\cosh\theta - e^{-2\lambda t}\sinh\theta\right).$$

By assumption, $m_N(0) \to m(0)$. Hence, for every $\theta \in \mathbb{R}$, the free energy $\Lambda^q_t(\theta) := \lim_{N\to\infty} \Lambda^q_{N,t}(\theta)$ exists and is given by the expression stated above. □

Theorem 1.4. *For fixed $t \geq 0$, the magnetization $m_N(t)$ satisfies a Large Deviation Principle with speed N and rate function*

$$I^q_t(x) = \sup_{\theta\in\mathbb{R}}\{\theta x - \Lambda^q_t(\theta)\}.$$

Equivalently,

$$\mathbb{P}\left[m_N(t) \approx x \mid \sigma(0)\right] \asymp e^{-NI^q_t(x)}.$$

Proof. Fix $t \geq 0$. By the previous proposition, the large deviation free energy of $m_N(t)$ is given by

$$\Lambda_t(\theta) = \lim_{N\to\infty} \frac{1}{N} \log \mathbb{E}\left[e^{N\theta m_N(t)}\right].$$

Note that since the spins take values in $\{-1, 1\}$, the random variables $m_N(t)$ are uniformly bounded. Hence the moment generating functions are finite for all $\theta \in \mathbb{R}$. Moreover, the function Λ^q_t is finite and differentiable on $\mathbb{R}$. Therefore, by the Gärtner-Ellis theorem [3, Theorem 2.3.6], the sequence $(m_N(t))_{N\geq 1}$ satisfies a Large Deviation Principle with speed N and rate function as

$$I^q_t(x) = \sup_{\theta\in\mathbb{R}} \left\{\theta x - \Lambda^q_t(\theta)\right\}.$$

That is, for suitable sets $A \subset [-1, 1]$,

$$\mathbb{P}\left[m_N(t) \in A \mid \sigma(0)\right] \asymp \exp\left(-N \inf_{x\in A} I^q_t(x)\right).$$

□

The rate function $I_t^q(x)$ quantifies the exponential cost of observing atypical magnetizations. Larger deviations from the deterministic trajectory correspond to exponentially unlikely events.

To obtain more information about the rate function, we study the maximizer in the rate function $I_t^q(x)$. Since Λ_t^q is differentiable and convex, the maximizer $\theta^*(x)$ is characterized by the critical point equation

$$x = (\Lambda_t^q)'(\theta^*(x)).$$

An explicit expression for the optimizer and the corresponding rate function is derived in Appendix A.

1.7.2 Annealed setting

In the quenched setting, probabilities are computed conditionally on the initial configuration $\sigma(0)$, so the large deviation behavior keeps memory of the microscopic initial state. We now consider the annealed setting, in which the initial spins are sampled independently with distribution given by

$$\mathbb{P}[\sigma_i(0) = +1] = p, \qquad \mathbb{P}[\sigma_i(0) = -1] = 1 - p,$$

for some $p \in [0, 1]$. The probability measure therefore includes both the randomness of the initial configuration and the subsequent spin-flip dynamics. This additional averaging leads to a simpler and more explicit large deviation functional.

Proposition 1.6. *For fixed $t \geq 0$, in the annealed setting, the large deviation free energy of $m_N(t)$ exists and is given by*

$$\Lambda_t^{an}(\theta) := \log\left(\cosh\theta + m(t)\sinh\theta\right),$$

where $m(t) = e^{-2\lambda t}m(0)$, with $m(0) = 2p - 1$, indicates the deterministic magnetization.

Proof. In the annealed setting, the initial magnetization is given by the law of large numbers, since $\mathbb{E}\left[\sigma_i(0)\right] = 2p - 1 =: m(0)$. Recalling equation (1.2), we obtain

$$\mathbb{P}\left[\sigma_i(t) = 1\right] = p\,\frac{1 + e^{-2\lambda t}}{2} + (1 - p)\,\frac{1 - e^{-2\lambda t}}{2} = \frac{1 + e^{-2\lambda t}\,m(0)}{2}.$$

Using the deterministic limit $m(t) = e^{-2\lambda t}\,m(0)$, we get

$$\mathbb{P}\left[\sigma_i(t) = 1\right] = \frac{1 + m(t)}{2}, \qquad \mathbb{P}\left[\sigma_i(t) = -1\right] = \frac{1 - m(t)}{2}.$$

Therefore,

$$\mathbb{E}[e^{\theta\sigma_i(t)}] = \frac{1+m(t)}{2}e^{\theta} + \frac{1-m(t)}{2}e^{-\theta} = \cosh\theta + m(t)\sinh\theta.$$

Since the spins are independent, we have

$$\mathbb{E}[e^{N\theta m_N(t)}] = \mathbb{E}\left[e^{\theta\sum_{i=1}^N \sigma_i(t)}\right] = \prod_{i=1}^N \mathbb{E}\left[e^{\theta\sigma_i(t)}\right] = \left(\cosh\theta + m(t)\sinh\theta\right)^N.$$

Hence,

$$\Lambda_t^{an}(\theta) := \lim_{N\to\infty}\frac{1}{N}\log\mathbb{E}\left[e^{N\theta m_N(t)}\right] = \log\left(\cosh\theta + m(t)\sinh\theta\right).$$

□

Theorem 1.5. *For fixed $t \geq 0$, the magnetization $m_N(t)$ satisfies a Large Deviation Principle with speed N and rate function*

$$I_t^{an}(x) = \sup_{\theta\in\mathbb{R}}\{\theta x - \Lambda_t^{an}(\theta)\}.$$

Equivalently,

$$\mathbb{P}\left[m_N(t) \approx x\right] \asymp e^{-NI_t^{an}(x)}.$$

Proof. The proof is identical to that of Theorem 1.4. Indeed, the limiting logarithmic moment generating function Λ_t^{an} is finite and differentiable on $\mathbb{R}$, since the spins are bounded. The conclusion therefore follows directly from the Gärtner-Ellis theorem. □

Proposition 1.7. *For fixed $t \geq 0$, the annealed rate function is given by $I_t^{an}(x) = +\infty$ for $|x| > 1$, and by*

$$I_t^{an}(x) = \frac{1+x}{2}\log\left(\frac{1+x}{1+m(t)}\right) + \frac{1-x}{2}\log\left(\frac{1-x}{1-m(t)}\right), \qquad \text{for } |x| < 1.$$

Proof. By the annealed Large Deviation Principle,

$$I_t^{an}(x) = \sup_{\theta\in\mathbb{R}}\left\{\theta x - \Lambda_t^{an}(\theta)\right\}.$$

For $|x| < 1$, the maximizer $\theta^*(x)$ satisfies $x = \left(\Lambda_t^{an}\right)'(\theta^*)$. We compute

$$\left(\Lambda_t^{an}\right)'(\theta) = \frac{\sinh\theta + m(t)\cosh\theta}{\cosh\theta + m(t)\sinh\theta} = \frac{\tanh\theta + m(t)}{1 + m(t)\tanh\theta}.$$

Therefore,

$$x = \frac{\tanh\theta^* + m(t)}{1 + m(t)\tanh\theta^*}.$$

Solving for $\tanh\theta^*$, we obtain

$$\tanh\theta^* = \frac{x - m(t)}{1 - m(t)x},$$

and hence

$$\theta^*(x) = \operatorname{arctanh}\left(\frac{x - m(t)}{1 - m(t)x}\right).$$

Substituting this maximizer into the Legendre transform gives

$$I_t^{an}(x) = x\theta^*(x) - \log\left(\cosh\theta^*(x) + m\sinh\theta^*(x)\right).$$

Using the identities

$$\operatorname{arctanh}(z) = \frac{1}{2}\log\left(\frac{1+z}{1-z}\right), \qquad \cosh\theta = \frac{1}{\sqrt{1-\tanh^2\theta}},$$

one obtains, after simplification, the desired expression. Finally, since $m_N(t) \in [-1, 1]$, values $|x| > 1$ are impossible, and therefore $I_t^{an}(x) = +\infty$ for $|x| > 1$. □

Remark 1.3. The annealed rate function can be recognized as the relative entropy (Kullback-Leibler divergence) between two Bernoulli distributions with parameters $\frac{1+x}{2}$ and $\frac{1+m(t)}{2}$. Indeed, $I_t^{an}(x)$ measures the exponential cost of observing an empirical fraction of positive spins corresponding to magnetization x, instead of the typical value $m(t)$.

The minimum of the rate function is attained at $x = m(t)$, where $I_t^{an}(m(t))$ takes value 0, reflecting that the typical macroscopic evolution carries no large deviation cost. As x moves away from $m(t)$, the rate function increases, showing that atypical magnetizations become exponentially unlikely as $N \to \infty$.

From a physical perspective, this entropy structure shows the loss of microscopic information in the annealed case: many microscopic spin configurations correspond to the same macroscopic magnetization, and the rate function quantifies the entropic cost of an atypical macroscopic state.

1.7.3 Comparison of the two regimes

We now compare the two cases. Since the quenched setting has a fixed initial microscopic configuration, while the annealed setting benefits from the randomness of the initial state, atypical magnetizations are expected to be more costly in the quenched setting.

Remark 1.4. For every $t \geq 0$ and every $x \in [-1, 1]$, the quenched rate function is always larger than or equal to the annealed rate function:

$$I_t^q(x) \geq I_t^{an}(x).$$

Indeed, write

$$p = \frac{1 + m(0)}{2},$$
$$A_+ = \cosh\theta + e^{-2\lambda t}\sinh\theta,$$
$$A_- = \cosh\theta - e^{-2\lambda t}\sinh\theta.$$

Then we have

$$\Lambda_t^q(\theta) = p\log A_+ + (1-p)\log A_-,$$
$$\Lambda_t^{an}(\theta) = \log\left(pA_+ + (1-p)A_-\right).$$

Since the logarithm is concave, Jensen's inequality gives

$$p\log A_+ + (1-p)\log A_- \leq \log\left(pA_+ + (1-p)A_-\right).$$

Taking Legendre transforms therefore yields

$$I_t^q(x) = \sup_{\theta\in\mathbb{R}}\{\theta x - \Lambda_t^q(\theta)\} \geq \sup_{\theta\in\mathbb{R}}\{\theta x - \Lambda_t^{an}(\theta)\} = I_t^{an}(x).$$

Finally, equality holds at the typical value $x = m(t)$, where both rate functions take value 0.

The inequality $I_t^q(x) \geq I_t^{an}(x)$ shows that atypical magnetizations are exponentially less likely in the quenched setting than in the annealed one. In the annealed case, the randomness of the initial configuration contributes to the fluctuation, increasing the number of microscopic configurations compatible with a given macroscopic deviation. By contrast, in the quenched setting the initial configuration is fixed, so the deviation must be generated entirely by the stochastic dynamics, leading to a higher large-deviation cost.

This difference becomes more pronounced for magnetizations far from the typical trajectory $m(t)$, where the system retains stronger memory of the initial state. As illustrated in Figure 1.2, the two rate functions coincide at the typical magnetization, where no large deviation occurs, and separate as

the deviation from equilibrium increases. Furthermore, we also see that their difference is zero at the deterministic value of the magnetization.

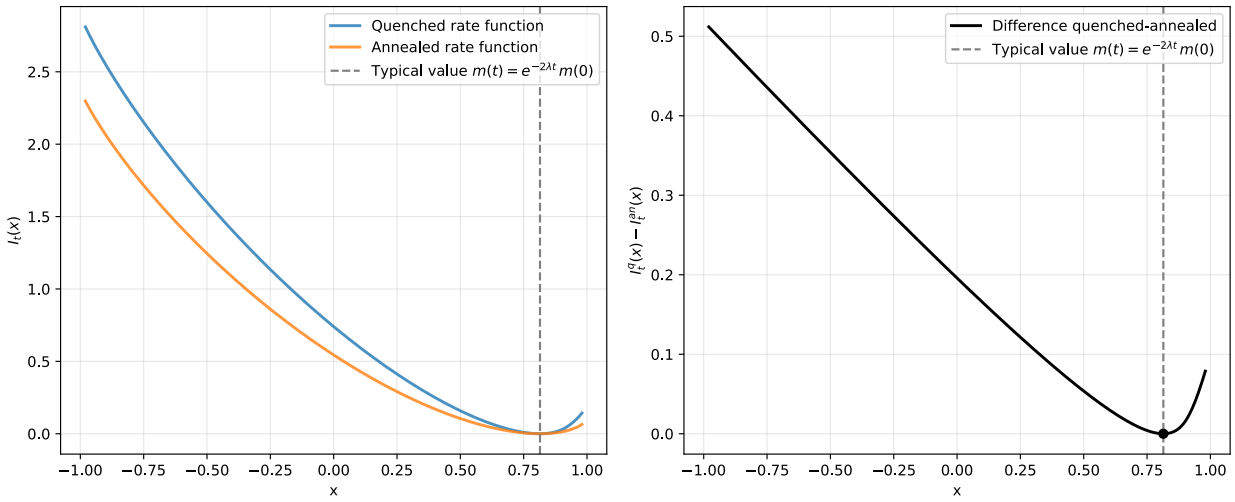

Figure 1.2: Comparison of the annealed and quenched rate functions $I_t(x)$ (left) and their difference $I_t^q(x) - I_t^{an}(x)$ (right), for chosen $m(0) = 0.9$, $t = 0.5$ and $\lambda = 0.1$. The minimum occurs at the typical value $m(t)$, where both rate functions vanish. The quenched rate function is consistently larger, as the additional constraint of the initial configuration increases the cost.

The results of this chapter describe three different scales of the same macroscopic observable. At the scale of the law of large numbers, the magnetization converges to the deterministic relaxation $m(t) = e^{-2\lambda t} m(0)$. At the scale of the central limit theorem, fluctuations around this relaxation are Gaussian and of order $N^{-1/2}$. At the large-deviation scale, order-one deviations from the typical magnetization become exponentially unlikely, with a cost described by the fixed-time rate functions derived above.

However, the fixed-time large deviation principle only answers part of the research question. It tells us how unlikely it is to observe an atypical magnetization at a prescribed time, but not how such a fluctuation is dynamically realized. Different microscopic evolutions may lead to the same final value of the magnetization. To identify the most likely macroscopic route to a rare fluctuation, we must therefore pass from fixed-time large deviations to a large deviation principle for entire trajectories.

Chapter 2

Rare trajectories of the magnetization

In this chapter, we study large deviations at the level of entire trajectories of the magnetization process. This leads to a variational description in terms of an action functional, analogous to the action in classical mechanics. The corresponding Hamiltonian structure allows us to characterize the optimal trajectories realizing rare macroscopic fluctuations [4].

2.1 Magnetization as a Markov process

We have already introduced the generator of the microscopic spin process. Before formulating the pathwise Large Deviation Principle for the magnetization, we first describe the Markov process relative to m_N.

Proposition 2.1. *The magnetization process $m_N(t)$ is a continuous-time Markov jump process on*

$$E_N = \left\{-1, -1 + \frac{2}{N}, \dots, 1 - \frac{2}{N}, 1\right\}.$$

Furthermore, its generator $\mathcal{L}_N$[1] acts on functions $f : E_N \to \mathbb{R}$ as

$$\mathcal{L}_N f(m) = \lambda N \frac{1-m}{2}\left[f\left(m + \frac{2}{N}\right) - f(m)\right] + \lambda N \frac{1+m}{2}\left[f\left(m - \frac{2}{N}\right) - f(m)\right].$$

Proof. Let $f : E_N \to \mathbb{R}$, and define a function F on the microscopic configuration space by $F(\sigma) = f(m_N(\sigma))$. Using the microscopic generator from

[1]For clarity, the notation $\mathcal{L}_N$ is used here for the generator of the magnetization Markov process, to avoid confusion with the previously defined generator L_N of the spin process.

equation (1.10), we obtain

$$L_N F(\sigma) = \sum_{i=1}^{N} \lambda \left[F\left(\sigma^i\right) - F\left(\sigma\right) \right],$$

where σ^i denotes the configuration obtained from σ by flipping the i-th spin. If $\sigma_i = -1$, then flipping this spin increases the magnetization by $2/N$, while if $\sigma_i = +1$, it decreases the magnetization by $2/N$. Therefore,

$$F(\sigma^i) = \begin{cases} f\left(m_N(\sigma) + \frac{2}{N}\right), & \sigma_i = -1, \\ f\left(m_N(\sigma) - \frac{2}{N}\right), & \sigma_i = +1. \end{cases}$$

Writing $m = m_N(\sigma)$, the numbers of positive and negative spins are

$$N_+ = N\frac{1+m}{2}, \qquad N_- = N\frac{1-m}{2}.$$

Hence

$$\begin{aligned} L_N F(\sigma) &= \lambda N_- \left[f\left(m + \frac{2}{N}\right) - f(m) \right] + \lambda N_+ \left[f\left(m - \frac{2}{N}\right) - f(m) \right] \\ &= \lambda N \frac{1-m}{2} \left[f\left(m + \frac{2}{N}\right) - f(m) \right] + \lambda N \frac{1+m}{2} \left[f\left(m - \frac{2}{N}\right) - f(m) \right]. \end{aligned}$$

Since the right-hand side depends on σ only through $m = m_N(\sigma)$, the magnetization process is a Markov process, with the given generator. □

Remark 2.1. The fact that the magnetization itself is a Markov process is a special feature of this model. Since the spins evolve independently, the jump rates depend only on the current numbers of positive and negative spins, which are completely determined by the magnetization.

In more general interacting spin systems, such as the Ising model with nearest-neighbor interactions, the evolution of a given spin depends on the local configuration of its neighbors [5]. In that case, two microscopic configurations with the same magnetization may evolve differently, and the magnetization alone is generally no longer a Markov process.

On the other hand, certain mean-field models still preserve this property. For instance, in the Curie-Weiss model, the spin flips depend on the total empirical magnetization. Then the induced dynamics of the magnetization again form a closed Markov process, with different transition rates than the ones above.

2.2 From fixed-time to pathwise large deviations

The fixed-time large deviation principle derived in the previous chapter quantifies the probability of observing an atypical value of the magnetization at a prescribed time. It gives an asymptotic estimate of the form

$$\mathbb{P}[X_N \approx x] \asymp e^{-NI(x)}.$$

To describe rare events dynamically, we need a large deviation principle on path space [6]. Instead of assigning a cost only to a final value x, the pathwise large deviation principle assigns a cost to an entire trajectory $\phi : [0,T] \to [-1,1]$. Informally, it has the form

$$\mathbb{P}(m_N(\cdot) \approx \phi(\cdot)) \asymp e^{-NI_{[0,T]}(\phi)}.$$

The functional $I_{[0,T]}$ is called the action functional. It measures the exponential cost of observing the macroscopic path ϕ. Typical trajectories have zero cost, while atypical trajectories have positive cost.

For Markov jump processes, the action functional is obtained through a Hamiltonian-Lagrangian structure. The starting point is the generator L_N of the process for finite N.

Definition 2.1. For a test function $\varphi : E_N \to \mathbb{R}$, we define the nonlinear generator of the magnetization

$$\mathcal{H}_N\varphi(m) = \frac{1}{N} e^{-N\varphi(m)} \cdot \mathcal{L}_N(e^{N\varphi})(m).$$

The nonlinear generator in the limit $N \to \infty$ gives a Hamiltonian $H(m,p)$. The variable m denotes the macroscopic state, while p is a conjugate variable. The corresponding Lagrangian is then defined by the Legendre transform

$$L(m,v) = \sup_{p \in \mathbb{R}} \{pv - H(m,p)\}.$$

Here v represents the velocity of the macroscopic trajectory. The pathwise rate functional is then given by

$$I_{[0,T]}(\phi) = \int_0^T L(\phi(t), \dot{\phi}(t))\, dt,$$

for sufficiently regular paths ϕ.

This structure is analogous to the variational formulation of classical mechanics, where trajectories are selected by minimizing an action. In the

present probabilistic setting, however, the action has a different interpretation: it measures the exponential cost of a fluctuation. Therefore, given an initial magnetization $m(0) = m_0$ and a final value $m(T) = x$, the most likely rare trajectory is expected to be the path minimizing $I_{[0,T]}$ among all paths connecting these endpoints.

2.3 Hamiltonian structure and large deviations

We can now apply the structure explained above to the magnetization process. Recalling the definition of the nonlinear generator $\mathcal{H}_N$, we derive the Hamiltonian.

Proposition 2.2. *In our model, for smooth test functions φ,*

$$\mathcal{H}_N\varphi(m) \to H(m, \varphi'(m))$$

as $N \to \infty$, where

$$H(m,p) = \lambda\frac{1-m}{2}(e^{2p}-1) + \lambda\frac{1+m}{2}(e^{-2p}-1). \tag{2.1}$$

Proof. Substituting the generator of the magnetization process in the nonlinear generator definition gives

$$\begin{aligned}\mathcal{H}_N\varphi(m) = \lambda\frac{1-m}{2}\left[\exp\left(N\left(\varphi\left(m+\frac{2}{N}\right)-\varphi(m)\right)\right)-1\right] \\ + \lambda\frac{1+m}{2}\left[\exp\left(N\left(\varphi\left(m-\frac{2}{N}\right)-\varphi(m)\right)\right)-1\right].\end{aligned}$$

Since φ is smooth, Taylor expansion around m yields

$$N\left(\varphi\left(m+\frac{2}{N}\right)-\varphi(m)\right) = 2\varphi'(m) + \mathcal{O}(N^{-1}),$$

and

$$N\left(\varphi\left(m-\frac{2}{N}\right)-\varphi(m)\right) = -2\varphi'(m) + \mathcal{O}(N^{-1}).$$

Therefore, as $N \to \infty$,

$$\exp\left(N\left(\varphi\left(m+\frac{2}{N}\right)-\varphi(m)\right)\right) \to e^{2\varphi'(m)},$$

and

$$\exp\left(N\left(\varphi\left(m-\frac{2}{N}\right)-\varphi(m)\right)\right)\to e^{-2\varphi'(m)}.$$

Substituting these limits gives

$$\mathcal{H}_N\varphi(m)\to\lambda\frac{1-m}{2}\left(e^{2\varphi'(m)}-1\right)+\lambda\frac{1+m}{2}\left(e^{-2\varphi'(m)}-1\right).$$

Writing $p=\varphi'(m)$, this is precisely the given Hamiltonian. □

To describe the cost of trajectories directly in terms of the magnetization $m(t)$ and its velocity $\dot{m}(t)$, we introduce the associated Lagrangian, defined as the Legendre transform of the Hamiltonian. An explicit expression of the Lagrangian is derived in Appendix B. Recall that in Section 1.7, the fixed-time rate function is derived from the Legendre transform of the large deviation free energy. Similarly, in the following proposition, we compute the pathwise rate functional from the Lagrangian.

Proposition 2.3. *Under suitable regularity assumptions, the probability that the magnetization trajectory $m_N(t)$ remains close to a sufficiently regular path $\phi:[0,T]\to[-1,1]$ behaves as*

$$\mathbb{P}\big(m_N(\cdot)\approx\phi(\cdot)\big)\asymp e^{-NI_{[0,T]}(\phi)},$$

where the rate functional is

$$I_{[0,T]}(\phi)=\int_0^T L(\phi(t),\dot{\phi}(t))\,dt.$$

Proof. The rigorous derivation of Proposition 2.3 follows from the general theory of large deviations for Markov processes developed by Feng and Kurtz [6]. We restrict ourselves here to the formal structure of the resulting rate functional. □

The rate functional $I_{[0,T]}(\phi)$ quantifies the exponential cost of observing a trajectory ϕ of the magnetization process. Paths with smaller value of $I_{[0,T]}$ are more likely to occur, while trajectories corresponding to large values become exponentially unlikely as $N\to\infty$. We therefore expect that the deterministic evolution, derived in Chapter 1, corresponds to the unique trajectory with zero cost.

Proposition 2.4. *For a given initial condition, the deterministic evolution $\dot{m}=-2\lambda m$, or, equivalently, $m(t)=e^{-2\lambda t}\,m(0)$, is the unique trajectory with zero rate functional.*

Proof. By definition of the Legendre transform, $L(m, v) \geq pv - H(m, p)$ for all $p \in \mathbb{R}$. Choosing $p = 0$ gives $L(m, v) \geq -H(m, 0) = 0$, since $H(m, 0) = 0$. Equality holds precisely when $v = \partial_p H(m, 0)$. Since

$$\partial_p H(m, p) = \lambda(1 - m)e^{2p} - \lambda(1 + m)e^{-2p},$$

we obtain $\partial_p H(m, 0) = -2\lambda m$. Therefore

$$L(m, -2\lambda m) = 0,$$

and consequently the deterministic trajectory is the unique zero-cost path. □

Remark 2.2. The theory of pathwise large deviations naturally leads to a structure formally analogous to classical mechanics, such as the concepts of Hamiltonian and Lagrangian.

The variable m plays the role of a position coordinate, while the conjugate variable p acts as a momentum. The rate functional $I_{[0,T]}(\phi)$ is analogous to the classical action. Trajectories minimizing the rate functional satisfy Hamilton equations associated with the Hamiltonian $H(m, p)$. This is formally the same variational structure that appears in classical mechanics, where extremal trajectories arise from Hamilton's principle [7].

Although the interpretation is probabilistic rather than mechanical, the mathematical structure is the same [8].

2.4 Optimal trajectories

The pathwise Large Deviation Principle provides not only the probability of observing atypical trajectories, but also a variational description of how such fluctuations are dynamically realized. Since each trajectory is assigned an exponential cost through the rate functional, rare events are expected to occur through paths minimizing this cost. More precisely, given an initial magnetization $m(0) = m_0$ and a final value $m(T) = x$, we look for the path ϕ minimizing

$$I_{[0,T]}(\phi) = \int_0^T L(\phi(t), \dot{\phi}(t))\, dt$$

among all sufficiently regular paths satisfying these boundary conditions.

The minimizers satisfy the Hamilton equations associated with the Hamiltonian $H(m, p)$:

$$\dot{m} = \partial_p H(m, p), \qquad \dot{p} = -\partial_m H(m, p).$$

For the spin-flip Hamiltonian this gives

$$\dot{m} = \lambda(1-m)e^{2p} - \lambda(1+m)e^{-2p}, \qquad \dot{p} = \lambda \sinh(2p).$$

An explicit expression for the optimal trajectory is given in the following proposition.

Proposition 2.5. *Let $m(0) = m_0$ and $m(T) = x$. The trajectory minimizing the pathwise rate functional is*

$$m(t) = \frac{m_0 \sinh\left(2\lambda(T-t)\right) + x \sinh(2\lambda t)}{\sinh(2\lambda T)}. \tag{2.2}$$

Proof. Optimal trajectories satisfy Hamilton's equations, as stated above. Differentiating the first equation for m gives

$$\begin{aligned}\ddot{m} &= -\lambda \dot{m} e^{2p} + 2\lambda(1-m)e^{2p}\dot{p} - \lambda \dot{m} e^{-2p} + 2\lambda(1+m)e^{-2p}\dot{p} \\ &= -\lambda \dot{m}(e^{2p} + e^{-2p}) + 2\lambda \dot{p}\left((1-m)e^{2p} + (1+m)e^{-2p}\right).\end{aligned}$$

After substituting the Hamilton equations for $\dot{m}$ and $\dot{p}$ and expanding the two products, all terms cancel except the ones proportional to m. This yields $\ddot{m} = 4\lambda^2 m$. Therefore the optimal trajectory satisfies the boundary value problem

$$\ddot{m} = 4\lambda^2 m, \qquad m(0) = m_0, \qquad m(T) = x.$$

The general solution is

$$m(t) = A \sinh(2\lambda t) + B \cosh(2\lambda t).$$

From $m(0) = m_0$, we get $B = m_0$. Imposing $m(T) = x$ gives

$$A = \frac{x - m_0 \cosh(2\lambda T)}{\sinh(2\lambda T)}.$$

Hence

$$m(t) = m_0 \cosh(2\lambda t) + \frac{x - m_0 \cosh(2\lambda T)}{\sinh(2\lambda T)} \sinh(2\lambda t).$$

Using the identity $\sinh(a-b) = \sinh(a)\cosh(b) - \cosh(a)\sinh(b)$, this can be rewritten as the desired expression. □

To check whether this result is consistent, we set the endpoint to be the typical value $x = e^{-2\lambda T} m_0$. Then the optimal trajectory reduces to

$m(t) = e^{-2\lambda t}\, m_0$. Thus the deterministic relaxation is recovered as the zero-cost optimal trajectory.

The explicit form of the optimal trajectories allows for a direct comparison between the deterministic relaxation and the most likely paths associated with atypical endpoints. Figure 2.1 shows several optimal trajectories for different prescribed final magnetizations. The trajectories are qualitatively described in the following remark.

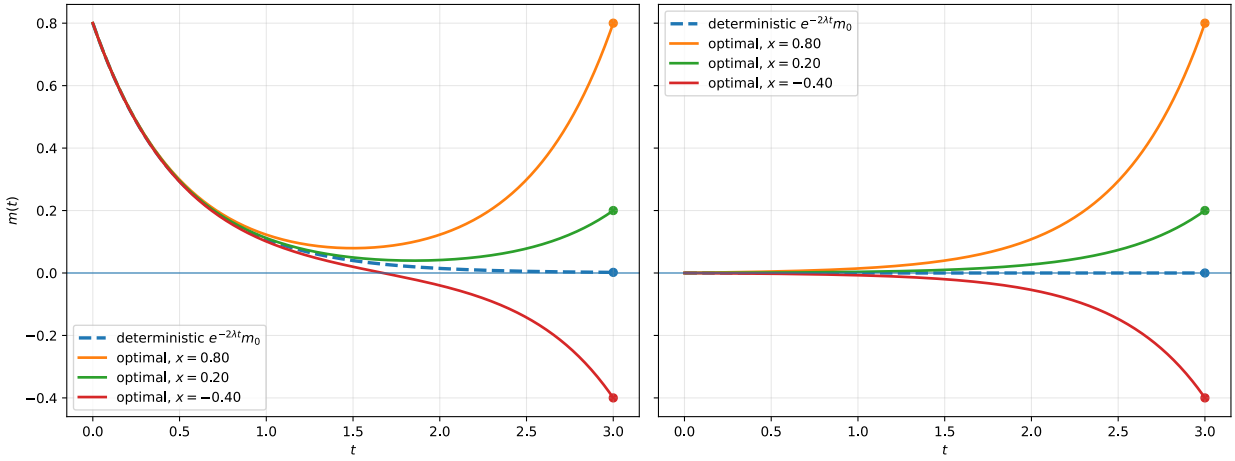

Figure 2.1: Optimal trajectories of the magnetization for different prescribed endpoints x at time $T = 3$, with $\lambda = 1$, compared with the deterministic relaxation $m(t) = e^{-2\lambda t} m_0$. Left: starting from $m_0 = 0.8$, the trajectories initially follow the deterministic decay toward equilibrium before deviating to reach the prescribed endpoint. Right: starting from equilibrium ($m_0 = 0$), the optimal trajectories remain close to zero for most of the interval and only deviate significantly near the final time.

Remark 2.3. The optimal trajectories initially remain close to the deterministic relaxation and only deviate significantly when necessary to reach the chosen endpoint. This reflects the dissipative nature of the dynamics: maintaining an atypical magnetization over a long time carries a larger cost than producing the fluctuation near the final time.

In particular, when the system starts close to equilibrium, as in the right plot of Figure 2.1, the optimal trajectories remain near equilibrium for most of the interval before deviating near the final time. If the chosen T is large enough, for any starting value m_0, all optimal trajectories first converge to the deterministic evolution.

2.5 Gaussian structure of the optimal trajectories

The explicit form of the optimal trajectories suggests a connection with Gaussian relaxation processes. To clarify this structure, we compare the spin-flip model with the Ornstein–Uhlenbeck process, whose optimal fluctuation trajectories satisfy the same second-order equation [9, 10]. This reveals that, although the Hamiltonian in our spin-flip model is nonlinear, the minimizing trajectories coincide with those of a Gaussian process.

Definition 2.2. The Ornstein–Uhlenbeck process is the stochastic process $X(t)$ satisfying the stochastic differential equation

$$dX(t) = -\kappa X(t)\,dt + \sigma dW(t), \tag{2.3}$$

where $\kappa > 0$ is the relaxation rate, $\sigma > 0$ determines the strength of the noise, and $W(t)$ is a standard Brownian motion.

The deterministic drift term $-\kappa X(t)$ drives the process exponentially toward equilibrium, while the stochastic term $\sigma dW(t)$ produces Gaussian fluctuations around this relaxation. We now repeat the derivation of the optimal trajectory for this process.

Proposition 2.6. *For the Ornstein–Uhlenbeck process, the optimal trajectory connecting $x(0) = x_0$ to $x(T) = x_T$ satisfies*

$$\ddot{x} = \kappa^2 x.$$

Therefore it is given by

$$x^*(t) = \frac{x_0 \sinh(\kappa(T-t)) + x_T \sinh(\kappa t)}{\sinh(\kappa T)}.$$

Proof. The generator of the Ornstein–Uhlenbeck process is

$$L = -\kappa x \partial_x + \frac{\sigma^2}{2}\partial_x^2.$$

Applying L to e^{Nf} gives

$$\partial_x e^{Nf} = Nf' e^{Nf}, \qquad \partial_x^2 e^{Nf} = \left(Nf'' + N^2 (f')^2\right) e^{Nf}.$$

Hence

$$\frac{1}{N} e^{-Nf} L(e^{Nf}) = -\kappa x f' + \frac{\sigma^2}{2}(f')^2 + \frac{\sigma^2}{2N} f''.$$

Taking the limit $N \to \infty$, we obtain the Hamiltonian

$$H(x,p) = -\kappa x p + \frac{\sigma^2}{2} p^2.$$

Hamilton's equations are

$$\dot{x} = \partial_p H(x,p) = -\kappa x + \sigma^2 p, \qquad \dot{p} = -\partial_x H(x,p) = \kappa p.$$

Differentiating the first equation and substituting $\dot{p} = \kappa p$ gives

$$\ddot{x} = -\kappa \dot{x} + \sigma^2 \kappa p = -\kappa(-\kappa x + \sigma^2 p) + \sigma^2 \kappa p = \kappa^2 x.$$

Therefore the optimal trajectories satisfy

$$\ddot{x} = \kappa^2 x, \qquad x(0) = x_0, \qquad x(T) = x_T.$$

Solving this boundary value problem yields

$$x^*(t) = \frac{x_0 \sinh(\kappa(T-t)) + x_T \sinh(\kappa t)}{\sinh(\kappa T)}.$$

□

Remark 2.4. The optimal trajectories of the Ornstein–Uhlenbeck process have the same form as the ones obtained in equation (2.2) for the spin-flip model. Indeed, the spin-flip trajectories satisfy $\ddot{m} = 4\lambda^2 m$, while the Ornstein–Uhlenbeck trajectories satisfy $\ddot{x} = \kappa^2 x$. Thus, the two boundary value problems coincide for $\kappa = 2\lambda$. Equivalently, the expressions for the optimal trajectory coincide.

This coincidence should not be interpreted as saying that the spin-flip large deviation principle is Gaussian. The Ornstein–Uhlenbeck Hamiltonian is quadratic, whereas the spin-flip Hamiltonian is non-quadratic. The agreement occurs at the level of the minimizing trajectories, not at the level of the full rate functional.

The Ornstein–Uhlenbeck process already appeared in the fluctuation theory developed in section 1.5. There, after centering around the deterministic magnetization and rescaling by $\sqrt{N}$, the fluctuation process converged to an Ornstein–Uhlenbeck process.

This comparison shows that the same structure also emerges at the level of optimal large-deviation trajectories. Thus the Ornstein–Uhlenbeck process plays a double role in the spin-flip model: it describes both the typical Gaussian fluctuations around equilibrium and the geometry of the optimal trajectories realizing rare fluctuations.

We conclude that rare macroscopic fluctuations are not realized through arbitrary stochastic evolutions, but through highly structured optimal trajectories determined by a variational principle. Although the underlying spin dynamics are random and microscopically reversible, the Large Deviation Principle selects specific trajectories which correspond to atypical macroscopic behavior.

Chapter 3

Beyond the independent spin-flip model

In the previous chapters, the independent spin-flip model provided a setting in which the emergence of macroscopic irreversibility could be studied explicitly. Because the spins evolve independently, the empirical magnetization forms a closed Markov process. This allowed us to derive its deterministic relaxation, describe its Gaussian fluctuations, and formulate a pathwise Large Deviation Principle in terms of a one-dimensional Hamiltonian and Lagrangian.

This tractability, however, is also a limitation of the model. The independent spin-flip system contains no spatial structure, no energetic interaction between neighboring spins, and no mechanism for the formation of domains or interfaces. Rare trajectories of the magnetization can therefore be understood as atypical outcomes of many independent local spin flips. In more realistic interacting systems, this picture is no longer sufficient.

The purpose of this chapter is to examine what changes when interactions are introduced. We use the two-dimensional Ising model as a qualitative extension of the independent spin-flip model. The aim is not to develop a full pathwise large deviation theory for the Ising model, but to identify the new mechanisms that appear once spins influence one another.

3.1 From independent spins to interacting systems

The analysis in the previous chapters relied on a special property of the independent spin-flip model: the empirical magnetization is itself a closed Markov process. Indeed, once the value of $m_N(t)$ is known, the number of

positive and negative spins is determined, and therefore the rates at which the magnetization jumps upward or downward are also determined. This closure allowed us to pass from the microscopic spin dynamics to an effective one-dimensional Markov process for $m_N(t)$.

This property is no longer available in general interacting spin systems. When the flip rate of a spin depends on its neighbors, the future evolution is not determined by the magnetization alone. Two microscopic configurations may have the same magnetization but very different spatial structures. For instance, one configuration may consist of a nearly random mixture of positive and negative spins, while another may contain two large ordered domains separated by a short interface. Although these configurations have the same value of m_N, they have different energies and different numbers of energetically favorable spin flips. Their subsequent evolution is therefore different.

The introduction of interactions therefore changes the mechanism behind both deterministic relaxation and fluctuations. In the independent model, relaxation towards equilibrium is essentially homogeneous: it results from the averaging of many independent spin flips, and rare deviations can be interpreted as atypical collective outcomes of these independent local events. In an interacting model, by contrast, relaxation may proceed through the formation, growth, and motion of spatial structures such as domains and interfaces. Domains are spatial regions in which many neighboring spins are aligned in the same direction, forming locally ordered $+1$ or -1 phases. Interfaces are the boundaries between such domains, where neighboring spins of opposite sign meet. Rare trajectories may then require the creation of energetically costly geometric objects, rather than only an atypical number of spin flips.

3.2 The two-dimensional Ising model with Glauber-type dynamics

To illustrate the effect of interactions, we consider the two-dimensional ferromagnetic Ising model on a square lattice [11]. Each lattice site i carries a spin $\sigma_i \in -1, +1$, and neighboring spins interact through the Hamiltonian

$$H(\sigma) = -J \sum_{\langle i,j \rangle} \sigma_i \sigma_j - h \sum_i \sigma_i,$$

where $J > 0$ is the ferromagnetic coupling strength, h is an external magnetic field, and $\langle i, j \rangle$ denotes nearest-neighbor pairs. The first term favors

alignment of neighboring spins, while the second term favors alignment with the external field.

The dynamics considered here are of Glauber type [12]. This means that the system evolves by single-spin flips: at each update, one spin is selected and may be flipped according to a probability depending on the corresponding change in energy. In contrast with conservative dynamics, such as Kawasaki dynamics, the total magnetization is not preserved. This makes Glauber dynamics a natural interacting analogue of the independent spin-flip model studied in the previous chapters.

If the spin at site i is flipped, the resulting configuration is denoted by σ^i, and the corresponding energy difference is

$$\Delta H_i(\sigma) = H(\sigma^i) - H(\sigma).$$

For the Ising Hamiltonian above, this energy difference is determined only by the spin σ_i, its nearest neighbors, and the external field. Explicitly,

$$\Delta H_i(\sigma) = 2\sigma_i \left(J \sum_{j \sim i} \sigma_j + h \right),$$

where the sum is over the nearest neighbors of i. Thus the flip probability is no longer independent of the surrounding configuration: a spin aligned with most of its neighbors is less likely to flip at low temperature than a spin located near an interface.

In the simulations below, Glauber-type dynamics is implemented using the Metropolis acceptance rule [13]. At each attempted update, a lattice site is chosen uniformly at random. If flipping the spin lowers the energy, the flip is accepted. If it increases the energy by $\Delta H_i > 0$, the flip is accepted with probability $e^{-\beta \Delta H_i}$, where $\beta = 1/T$ is the inverse temperature. Equivalently, the acceptance probability is

$$\mathbb{P}_{\text{acc}}\left[\sigma_i \to -\sigma_i\right] = \min\{1, e^{-\beta \Delta H_i}\}. \tag{3.1}$$

This dynamics is reversible with respect to the Gibbs distribution associated with the Ising Hamiltonian.

The simulations were performed on a square lattice of size $L \times L$ with periodic boundary conditions. Periodic boundary conditions reduce boundary effects by identifying opposite edges of the lattice, so that each spin has four nearest neighbors. One unit of simulation time is taken to be one Monte Carlo sweep, consisting of L^2 attempted single-spin updates. During the simulation, both the magnetization $m_N(\sigma)$ and the energy per spin $H(\sigma)/N$ are recorded.

The numerical procedure can be summarized as follows:

1. Initialize an $L \times L$ spin configuration.
2. Choose a lattice site i uniformly at random.
3. Compute the energy difference $\Delta H_i = H(\sigma^i) - H(\sigma)$.
4. Accept the flip if $\Delta H_i \leq 0$.
5. If $\Delta H_i > 0$, accept the flip with probability $e^{-\beta \Delta H_i}$.
6. Repeat this procedure L^2 times for one Monte Carlo sweep.
7. Record the magnetization and energy, and continue for the desired number of sweeps.

The purpose of these simulations is not to perform a systematic numerical study of the Ising model, but to illustrate the qualitative mechanisms introduced by interactions. In particular, they show how relaxation and rare transitions are shaped by spatial structures such as domains and interfaces, which are clearly absent from the independent spin-flip model.

3.3 Domain formation and collective relaxation

We first consider the Ising model with zero external field, $h = 0$, starting from a disordered initial configuration in which the spins are chosen independently with equal probability of being $+1$ or -1. This initial state has magnetization close to zero, but it is not an equilibrium configuration at low temperature. Indeed, below the critical temperature, the ferromagnetic interaction favors ordered phases in which most spins are aligned.

The qualitative behavior depends strongly on the temperature. For the two-dimensional Ising model on the square lattice, the critical temperature is given by Onsager's exact solution [14],

$$T_c = \frac{2J}{k_B \log(1 + \sqrt{2})}. \tag{3.2}$$

In the units used in the simulations, we set $J = k_B = 1$, and therefore $T_c \approx 2.27$. We compare a low-temperature evolution with $T < T_c$ to a high-temperature evolution with $T > T_c$.

At low temperature, neighboring spins tend to align and the system progressively develops ordered regions, the domains. The boundaries between

domains are the interfaces. Interfaces contain neighboring spins of opposite sign and therefore contribute positively to the energy. As the dynamics evolves, the system lowers its energy by reducing the total length of these interfaces. This produces a coarsening process in which small domains disappear and larger domains grow.

This mechanism is fundamentally different from the relaxation observed in the independent spin-flip model. In the independent model, each spin evolves without regard to its neighbors, and the deterministic relaxation of the magnetization results from averaging many independent random flips. In the interacting Ising model, by contrast, the evolution is spatially organized. A spin located inside a large aligned domain is unlikely to flip at low temperature, because doing so would create several disagreeing neighbor pairs. A spin near an interface, however, may flip more easily if this shortens the boundary between domains. Relaxation is therefore driven not only by the number of positive and negative spins, but also by their spatial arrangement.

This collective mechanism is visible in Figure 3.1. Starting from a disordered configuration, the low-temperature dynamics produces increasingly large domains. The system does not relax through independent local fluctuations distributed uniformly across the lattice, but through the motion and elimination of interfaces. At high temperature, thermal fluctuations dominate over the aligning interaction, and stable macroscopic domains do not form. The system remains disordered on large scales, and the magnetization fluctuates around zero.

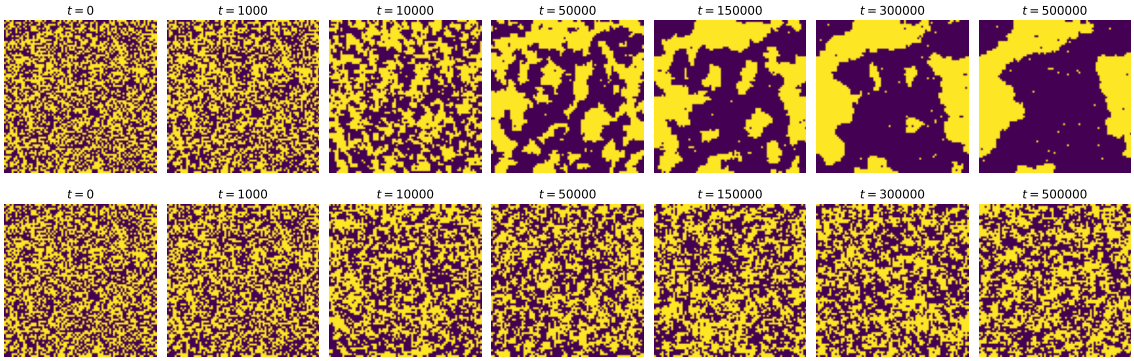

Figure 3.1: Time evolution of the two-dimensional Ising model starting from a disordered initial configuration. Top: low-temperature dynamics, where ferromagnetic interactions dominate thermal fluctuations and large ordered domains progressively emerge. Bottom: high-temperature dynamics, where thermal fluctuations prevent long-range ordering and the system remains macroscopically disordered.

The same distinction appears in the macroscopic observables shown in Figure 3.2. At low temperature, the energy per spin decreases as neighboring spins become increasingly aligned and the total interface length is reduced. The magnetization moves away from its initially small value as one of the two ordered phases becomes dominant. Since $h = 0$, the Hamiltonian is symmetric under the global transformation $\sigma_i \mapsto -\sigma_i$. The choice of a positive or negative final magnetization is therefore not imposed by an external field, but selected dynamically from the initial fluctuations. This is an example of spontaneous symmetry breaking.

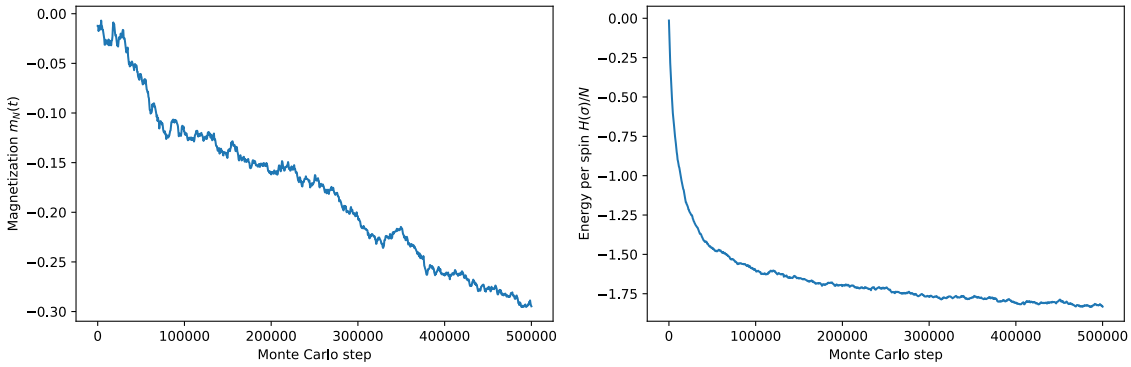

Figure 3.2: Macroscopic magnetization and energy per spin during the low-temperature evolution of the Ising model. The system progressively relaxes towards an ordered magnetized phase. As neighboring spins align and domains form, the system evolves towards lower-energy configurations.

It is an important point that the relaxation is no longer described by a closed deterministic equation for the magnetization alone. The magnetization records the average spin, but it does not record the amount of interface or the geometry of the domains. Two configurations may have the same magnetization and very different energies, depending on whether the spins are randomly mixed or organized into large domains. Interactions therefore turn macroscopic relaxation into a collective spatial process. This is precisely the feature that is absent in the independent spin-flip model and that becomes essential when studying rare trajectories in interacting systems.

3.4 Metastability as rare trajectories

The previous sections show that interactions make relaxation a collective spatial process. This becomes especially important when studying rare transitions. In the independent spin-flip model, an atypical trajectory of the

magnetization is produced by an unlikely collective outcome of many independent spin flips. In the interacting Ising model, rare transitions are instead shaped by the formation and growth of spatial structures. Metastability provides a clear example of this difference.

Metastability occurs when the system remains for a long time in a state that is locally stable but not globally stable [15]. In the Ising model, this can be observed at low temperature in the presence of a small external field. Suppose, for instance, that $h > 0$, so that the positively magnetized phase is energetically favored. If the system is initialized close to the negatively magnetized phase, then it is not at equilibrium. Nevertheless, at low temperature it may remain trapped near this negatively magnetized state for a long time. The reason is that leaving this state requires a sufficiently large collective fluctuation.

The transition does not occur by spins flipping independently and uniformly throughout the lattice. Instead, small droplets of the stable phase appear due to thermal fluctuations. We call droplet a small connected region of spins belonging to one phase inside the opposite phase. Most of these droplets disappear quickly: if a droplet is too small, the energetic cost of creating its boundary is larger than the energetic gain obtained by aligning its spins with the external field. Only when a droplet exceeds a critical size does it become favorable for it to grow. After such a critical droplet has formed, the stable phase expands rapidly and the system undergoes a sudden macroscopic transition.

From the large-deviation perspective, the formation of this critical droplet is the rare event that enables the transition. The system does not need to create the final stable phase all at once. Instead, it must first overcome an energetic barrier by producing a spatial fluctuation of the right size and shape. Once this barrier has been crossed, the subsequent growth of the stable phase is comparatively likely and proceeds through interface motion.

The metastable transition is illustrated in Figure 3.3. The system is initialized close to the negatively magnetized phase while the external field favors positive magnetization. For a long time, the system remains near the metastable state. During this period, small positive droplets may appear and disappear. Eventually, a sufficiently large droplet forms. Once this happens, the positively magnetized phase invades the system and the magnetization changes rapidly. The observed trajectory therefore consists of a long waiting time followed by a sudden transition.

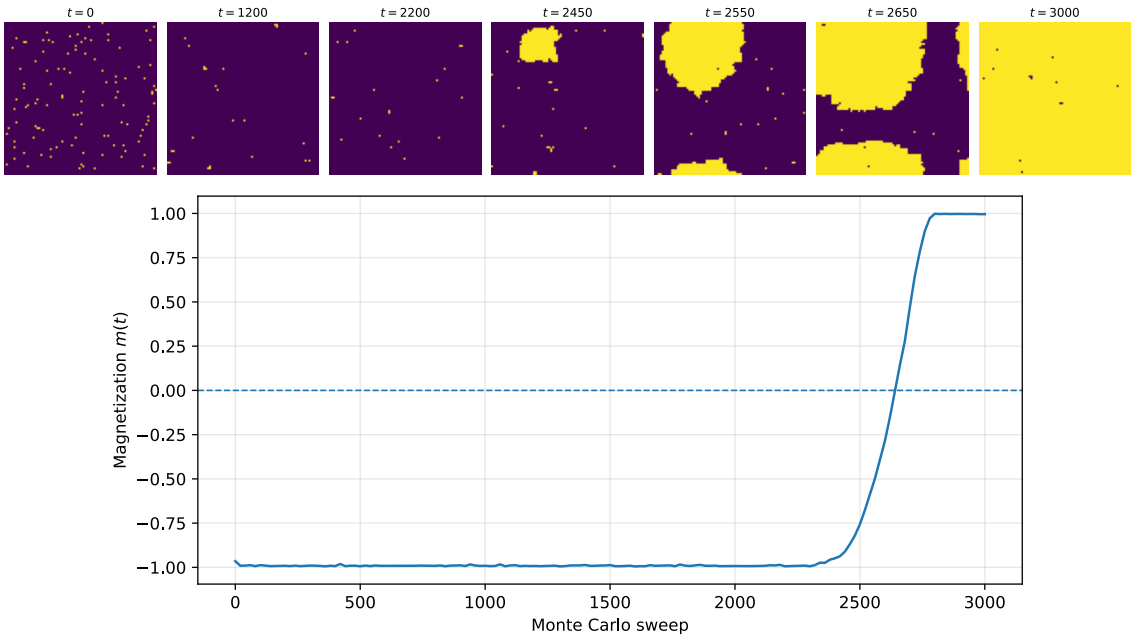

Figure 3.3: Metastable transition in the low-temperature Ising model under a weak external field favoring positive magnetization. The system is initialized close to the negatively magnetized phase and once a sufficiently large critical droplet is formed, the positively magnetized phase rapidly invades the system, leading to a sudden macroscopic transition.

In the independent spin-flip model, rare trajectories are costly because many independent random events must collectively produce an atypical magnetization. In the interacting Ising model, rare trajectories are costly because the system must create spatial structures that overcome interface and energy barriers. Thus metastability shows that, in interacting systems, large deviations are not only about how far the magnetization moves away from its typical value, but also about the geometric mechanism through which this movement is realized.

3.5 Consequences for the thesis question

The interacting Ising model is an example that the large-deviation picture developed for the independent spin-flip model captures only part of the general mechanism behind rare macroscopic trajectories. In the independent model, the empirical magnetization is a sufficient macroscopic variable: its evolution is Markovian, its deterministic relaxation can be derived explicitly,

and rare trajectories can be described through a one-dimensional Hamiltonian and Lagrangian structure.

Once interactions are introduced, this simplification is no longer available. The magnetization remains an important observable, but it does not contain enough information to determine the future evolution of the system. Spatial organization becomes relevant. Domains, interfaces, and droplets affect both the energetic cost and the dynamical realization of a fluctuation.

This suggests that, for interacting systems, a more complete large-deviation description should involve richer macroscopic variables than the total magnetization. Possible choices include empirical density profiles, which record how the spin distribution varies in space, or variables describing the geometry of interfaces between phases. In metastable regimes, one may also need to describe the formation and growth of critical droplets, since these objects determine the transition from a metastable phase to the stable one.

A natural direction for further study would therefore be to replace the scalar magnetization $m_N(t)$ by a spatially resolved observable. For example, instead of recording only the average spin over the whole lattice, one could study an empirical magnetization profile that assigns a local average magnetization to each region of space. Such a description would retain information about domains and interfaces, and could provide a more suitable framework for pathwise large deviations in interacting systems.

Another possible direction is the study of metastable transition times. In the independent spin-flip model, rare trajectories are described through an action cost for paths of the magnetization. In the low-temperature Ising model, the relevant rare event is the formation of a critical droplet. A quantitative theory would aim to estimate the exponential scale of the expected transition time and to characterize the most likely transition mechanism. This would connect the pathwise large-deviation viewpoint of Chapter 2 with the theory of metastability in interacting particle systems.

The main lesson is that the independent spin-flip model is not merely a toy model, but an exactly solvable reference case. It shows how macroscopic irreversibility and rare trajectories can be quantified. The interacting Ising model then reveals what must be added in more realistic systems. Thus, while the reverse microscopic evolutions remain possible, the way in which they become exponentially unlikely depends strongly on the microscopic structure of the model.

Conclusion

The aim of this thesis was to understand how irreversible macroscopic relaxation can arise from microscopic spin dynamics, and how rare trajectories opposing this relaxation can be described quantitatively. The independent spin-flip model provided a tractable setting in which this question could be answered explicitly.

The first main result is that the magnetization becomes deterministic in the thermodynamic limit. Although each spin evolves randomly and reversibly, the magnetization converges to the trajectory

$$m(t) = e^{-2\lambda t} m(0),$$

which relaxes irreversibly towards equilibrium. This shows how a preferred macroscopic direction in time can arise from symmetric microscopic dynamics: the randomness of individual flips averages out, while the overwhelming number of microscopic configurations near zero magnetization drives the macroscopic relaxation. Around this deterministic limit, fluctuations of order $N^{-1/2}$ converge to a Gaussian process, which can be identified with an Ornstein–Uhlenbeck process started from zero. Thus, the typical behavior of the system is described by deterministic relaxation, with Gaussian fluctuations around it.

Large deviation theory then gives a description of fluctuations beyond the Gaussian regime. Order-one deviations of the magnetization from its deterministic value occur with probabilities that are exponentially small in N, and the corresponding exponential cost is described by a rate function. A distinction appears between the quenched and annealed settings. In the quenched setting, the initial microscopic configuration is fixed, so an atypical magnetization at a later time must be produced entirely by the stochastic dynamics. In the annealed setting, the initial value of each spin is Bernoulli distributed, giving the system an additional source of fluctuation. This leads to the inequality

$$I_t^q(x) \geq I_t^{an}(x),$$

with equality at the typical value $x = m(t)$. The comparison shows that

rare macroscopic fluctuations retain information about how the microscopic initial condition is treated.

The fixed-time large deviation principle describes the cost of ending at an atypical magnetization, but not the way in which such a fluctuation is reached. The pathwise large deviation principle fills this gap by assigning an action cost to entire magnetization trajectories. In this formulation, the limiting nonlinear generator gives rise to a Hamiltonian, while the associated Lagrangian defines the rate functional. Rare trajectories are therefore selected by a variational principle: among all paths connecting prescribed endpoints, the most likely one minimizes this action. For the considered model, these optimal trajectories can be computed explicitly and satisfy the same second-order equation as the optimal paths of an Ornstein–Uhlenbeck process with relaxation rate 2λ. This agreement should not be interpreted as saying that the full spin-flip large deviation principle is Gaussian. It shows that the geometry of the minimizing trajectories has a Gaussian relaxation structure, even though the full Hamiltonian remains non-quadratic.

The final chapter shows why the independent model should be viewed as a tractable starting point rather than a complete picture of macroscopic irreversibility. In the two-dimensional Ising model, interactions introduce spatial correlations, domains and energy barriers. As a result, relaxation is no longer a homogeneous averaging process, and rare macroscopic transitions are no longer realized by independent local flips. In interacting systems, the relevant large-deviation cost cannot be captured by the final magnetization alone, but must also depend on the spatial organization of the spins.

Taken together, these results show that macroscopic irreversibility does not arise because the microscopic reverse trajectories are impossible. They remain possible, but their probability becomes exponentially small in the system size. Large deviation theory makes this statement quantitative: it identifies both the exponential cost of rare entropy-decreasing fluctuations and the most likely trajectories through which such fluctuations occur.

A limitation of the present analysis is that the pathwise large deviation structure was derived explicitly only for the independent spin-flip model, where the magnetization is itself a Markov process. In interacting systems such as the Ising model, the magnetization alone does not generally contain enough information to determine the future evolution. A natural continuation would therefore be to study large deviations for richer macroscopic variables, such as empirical density profiles or interfaces, which can capture the spatial mechanisms responsible for metastable transitions.

Thus, large deviation theory does not contradict microscopic reversibility. Instead, it explains how irreversible macroscopic behavior emerges statistically: trajectories opposing relaxation remain possible, but their probability

is exponentially suppressed, and their most likely realization is shaped by the microscopic structure of the model.

Bibliography

[1] Daniel Stroock. *Mathematics of Probability*. Vol. 149. American Mathematical Society, 2013.

[2] Stewart N. Ethier and Thomas G. Kurtz. *Markov Processes: Characterization and Convergence*. John Wiley & Sons, Ltd, 1986.

[3] Amir Dembo and Ofer Zeitouni. *Large deviations techniques and applications*. Springer, 2009.

[4] Vitalii Konarovskyi. "An Introduction to Large Deviations". Lecture notes. 2021. URL: https://www.math.uni-hamburg.de/forschung/bereiche/st/stopro/personen/konarovskyi-vitalii/dokumente/ldp.pdf.

[5] Thomas M. Liggett. *Interacting particle systems*. Springer, 1985.

[6] Jin Feng and Thomas G. Kurtz. *Large Deviations for Stochastic Processes*. American Mathematical Soc., 2006.

[7] John R. Taylor. *Classical mechanics*. University Science Books, 2005.

[8] Mark Freidlin and Alexander Wentzell. *Random perturbations of dynamical systems*. Springer, 2012.

[9] Frank Redig and Feijia Wang. "Gibbs-non-Gibbs transitions via large deviations: computable examples". In: *Journal of Statistical Physics* 147.6 (2012), pp. 1094–1112. DOI: 10.1007/s10955-012-0523-9.

[10] Crispin W. Gardiner. *Stochastic methods: a handbook for the natural and social sciences*. Springer, 2009.

[11] Julia M. Yeomans. *Statistical mechanics of phase transitions*. Oxford University Press, 1992.

[12] Roy J. Glauber. "Time-Dependent Statistics of the Ising Model". In: *Journal of Mathematical Physics* 4.2 (1963), pp. 294–307. DOI: 10.1063/1.1703954.

[13] Nicholas Metropolis et al. “Equation of State Calculations by Fast Computing Machines”. In: *The Journal of Chemical Physics* 21.6 (1953), pp. 1087–1092. DOI: 10.1063/1.1699114.

[14] Lars Onsager. “Crystal statistics. I. A two-dimensional model with an order-disorder transition”. In: *Physical Review* 65.3–4 (1944), pp. 117–149. DOI: 10.1103/PhysRev.65.117.

[15] Anton Bovier and Frank den Hollander. *Metastability: a potential-theoretic approach*. Springer, 2015.

Acknowledgements

I would like to thank Prof.dr. F.H.J. Redig and Prof.dr. S. Stallinga for their supervision, feedback, and guidance throughout this project.

The code used to generate the numerical simulations and figures in this thesis is available at this GitHub repository.[1] Generative AI tools were used to assist with code drafting, debugging, and formatting. All code was reviewed, adapted, and tested by the author, who remains responsible for the correctness of the simulations and figures.

[1] https://github.com/leo-cazzaniga/spin-flip-large-deviations-thesis

Appendix A
Explicit expression of the quenched rate function

In this appendix, we derive an explicit expression for the quenched rate function $I_t^q(x)$ introduced in Section 1.7.1. To reduce notation, we neglect the superscript q in the quenched rate function and moment generating function.

The rate function is defined through the Legendre transform

$$I_t(x) = \sup_{\theta \in \mathbb{R}} \{\theta x - \Lambda_t(\theta)\},$$

where

$$\Lambda_t(\theta) = \frac{1+m(0)}{2} \log\left(\cosh\theta + e^{-2\lambda t}\sinh\theta\right) + \frac{1-m(0)}{2}\log\left(\cosh\theta - e^{-2\lambda t}\sinh\theta\right).$$

The maximizer $\theta^*(x)$ is determined by the critical point equation $x = \Lambda_t'(\theta)$. Introducing $u = \tanh\theta$, this equation can be rewritten as

$$x = \frac{(1-e^{-4\lambda t})u + e^{-2\lambda t}m(0)(1-u^2)}{1-e^{-4\lambda t}u^2}.$$

This leads to the quadratic equation

$$\left(e^{-4\lambda t}x - e^{-2\lambda t}m(0)\right)u^2 + \left(1-e^{-4\lambda t}\right)u + \left(e^{-2\lambda t}m(0) - x\right) = 0.$$

Solving for u, and selecting the branch such that $u^*(x) = 0$ when $x = m(t) = e^{-2\lambda t}m(0)$, we obtain

$$u^*(x) = \frac{2\left(x - e^{-2\lambda t}m(0)\right)}{1-e^{-4\lambda t} + \sqrt{(1-e^{-4\lambda t})^2 + 4e^{-4\lambda t}\left(m(0)^2 + x^2\right) - 4e^{-2\lambda t}(1+e^{-4\lambda t})m(0)x}}.$$

The rate function is then given by

$$I_t(x) = x\,\mathrm{arctanh}(u^*) + \frac{1}{2}\log(1-(u^*)^2) - \frac{1+m(0)}{2}\log(1+e^{-2\lambda t}u^*) - \frac{1-m(0)}{2}\log(1-e^{-2\lambda t}u^*),$$

which yields the explicit expression, with the notation m_0 for $m(0)$:

$$I_t(x) = x \operatorname{arctanh}\left(\frac{2\left(x - e^{-2\lambda t} m_0\right)}{1 - e^{-4\lambda t} + \sqrt{(1 - e^{-4\lambda t})^2 + 4e^{-4\lambda t}\left(m_0^2 + x^2\right) - 4e^{-2\lambda t}(1 + e^{-4\lambda t}) m_0 x}}\right)$$
$$+ \frac{1}{2}\log\left(1 - \left[\frac{2\left(x - e^{-2\lambda t} m_0\right)}{1 - e^{-4\lambda t} + \sqrt{(1 - e^{-4\lambda t})^2 + 4e^{-4\lambda t}\left(m_0^2 + x^2\right) - 4e^{-2\lambda t}(1 + e^{-4\lambda t}) m_0 x}}\right]^2\right)$$
$$- \frac{1 + m_0}{2}\log\left(1 + e^{-2\lambda t}\frac{2\left(x - e^{-2\lambda t} m_0\right)}{1 - e^{-4\lambda t} + \sqrt{(1 - e^{-4\lambda t})^2 + 4e^{-4\lambda t}\left(m_0^2 + x^2\right) - 4e^{-2\lambda t}(1 + e^{-4\lambda t}) m_0 x}}\right)$$
$$- \frac{1 - m_0}{2}\log\left(1 - e^{-2\lambda t}\frac{2\left(x - e^{-2\lambda t} m_0\right)}{1 - e^{-4\lambda t} + \sqrt{(1 - e^{-4\lambda t})^2 + 4e^{-4\lambda t}\left(m_0^2 + x^2\right) - 4e^{-2\lambda t}(1 + e^{-4\lambda t}) m_0 x}}\right).$$

Although this expression is fully explicit, its complexity limits a direct interpretation. The implicit formulation via the Legendre transform is often more suitable for analytical purposes, while the explicit form can be useful for numerical evaluation.

Appendix B
Explicit expression of the Lagrangian

In this appendix, we derive the corresponding explicit expression for $L(m, v)$, as defined in Section 2.3.

Let

$$a = \lambda \frac{1-m}{2}, \qquad b = \lambda \frac{1+m}{2}.$$

Then the Hamiltonian can be written as

$$H(m, p) = a(e^{2p} - 1) + b(e^{-2p} - 1).$$

To compute the Legendre transform, we maximize $pv - H(m, p)$ with respect to p. The maximizer satisfies $v = \partial_p H(m, p)$. Since

$$\partial_p H(m, p) = 2ae^{2p} - 2be^{-2p},$$

the optimal value p^* is determined by

$$v = 2ae^{2p^*} - 2be^{-2p^*}.$$

Introducing $y = e^{2p^*}$, we obtain the quadratic equation

$$v = 2ay - \frac{2b}{y} \quad \Longrightarrow \quad 2ay^2 - vy - 2b = 0.$$

Since $y > 0$, the relevant solution is

$$y = \frac{v + \sqrt{v^2 + 16ab}}{4a}.$$

Substituting the values of a and b, we have

$$16ab = 4\lambda^2(1 - m^2),$$

and therefore

$$e^{2p^*} = \frac{v + \sqrt{v^2 + 4\lambda^2(1-m^2)}}{2\lambda(1-m)}.$$

Hence

$$p^* = \frac{1}{2}\log\left(\frac{v + \sqrt{v^2 + 4\lambda^2(1-m^2)}}{2\lambda(1-m)}\right).$$

We now evaluate the Legendre transform at this maximizer. Let

$$D(m,v) = \sqrt{v^2 + 4\lambda^2(1-m^2)}.$$

Using the relation $v = 2ae^{2p^*} - 2be^{-2p^*}$, one obtains

$$ae^{2p^*} = \frac{v + D(m,v)}{4}, \qquad be^{-2p^*} = \frac{D(m,v) - v}{4}.$$

Therefore,

$$H(m,p^*) = ae^{2p^*} + be^{-2p^*} - a - b = \frac{D(m,v)}{2} - \lambda.$$

Consequently,

$$L(m,v) = p^* v - H(m,p^*),$$

which gives

$$L(m,v) = \frac{v}{2}\log\left(\frac{v + \sqrt{v^2 + 4\lambda^2(1-m^2)}}{2\lambda(1-m)}\right) - \frac{1}{2}\sqrt{v^2 + 4\lambda^2(1-m^2)} + \lambda.$$

Although this expression is explicit, it is not particularly transparent. For this reason, the main text works mostly with the Hamiltonian and the Legendre-transform definition of the Lagrangian. The explicit form above is useful mainly when one wants to evaluate the pathwise cost $I_{[0,T]}(\phi)$ directly.

Appendix C
Spin-flip dynamics in an external field

In the independent spin-flip model studied throughout the thesis, positive and negative magnetizations are dynamically equivalent. The deterministic relaxation is symmetric around zero magnetization, and rare fluctuations towards positive and negative values carry the same large-deviation cost. We now briefly discuss a simple extension in which this symmetry is broken through the introduction of an external magnetic field.

The purpose of this appendix is to illustrate how a preferred macroscopic direction modifies both the deterministic relaxation and the geometry of rare fluctuations.

Each spin $\sigma_i(t) \in \{-1, +1\}$ evolves as an independent continuous-time Markov process with transition rates

$$c(-1, +1) = \lambda e^{\beta h}, \qquad c(+1, -1) = \lambda e^{-\beta h},$$

where $\lambda > 0$ is the flip rate parameter, $\beta > 0$ is the inverse temperature, and $h \in \mathbb{R}$ denotes the external magnetic field. For $h = 0$, the symmetric spin-flip model studied in this thesis is recovered.

Proposition C.1. *In the presence of an external field, the magnetization process $m_N(t)$ is a continuous-time Markov jump process on*

$$E_N = \left\{-1, -1 + \frac{2}{N}, \ldots, 1 - \frac{2}{N}, 1\right\}.$$

Its generator L_N^h acts on functions $f : E_N \to \mathbb{R}$ as

$$\begin{aligned}[L_N^h f](m) = {} & \lambda e^{\beta h} N \frac{1-m}{2} \left[f\left(m + \frac{2}{N}\right) - f(m) \right] \\ & + \lambda e^{-\beta h} N \frac{1+m}{2} \left[f\left(m - \frac{2}{N}\right) - f(m) \right].\end{aligned}$$

Proof. A flip from -1 to $+1$ increases the magnetization by $2/N$, while a flip from $+1$ to -1 decreases it by $2/N$. If the magnetization equals m, then the fractions of negative and positive spins are $(1-m)/2$ and $(1+m)/2$, respectively. The corresponding jump rates are therefore

$$m \mapsto m + \frac{2}{N} \quad \text{at rate} \quad \lambda e^{\beta h} N \frac{1-m}{2},$$

and

$$m \mapsto m - \frac{2}{N} \quad \text{at rate} \quad \lambda e^{-\beta h} N \frac{1+m}{2}.$$

Substituting these jumps into the generator yields the stated expression. □

Using the nonlinear generator

$$[H_N \phi](m) = \frac{1}{N} e^{-N\phi(m)} L_N^h(e^{N\phi})(m),$$

one obtains the limiting Hamiltonian.

Proposition C.2. *The limiting Hamiltonian associated with the magnetization process is*

$$H^h(m,p) = \lambda e^{\beta h} \frac{1-m}{2}(e^{2p}-1) + \lambda e^{-\beta h} \frac{1+m}{2}(e^{-2p}-1).$$

Proof. Substituting the generator into the nonlinear-generator definition gives

$$\begin{aligned}[H_N \phi](m) = {} & \lambda e^{\beta h} \frac{1-m}{2} \left[\exp\left(N \left(\phi\left(m + \frac{2}{N} \right) - \phi(m) \right) \right) - 1 \right] \\ & + \lambda e^{-\beta h} \frac{1+m}{2} \left[\exp\left(N \left(\phi\left(m - \frac{2}{N} \right) - \phi(m) \right) \right) - 1 \right].\end{aligned}$$

Since ϕ is smooth,

$$\begin{aligned} N \left(\phi\left(m + \frac{2}{N} \right) - \phi(m) \right) &= 2\phi'(m) + O(N^{-1}), \\ N \left(\phi\left(m - \frac{2}{N} \right) - \phi(m) \right) &= -2\phi'(m) + O(N^{-1}). \end{aligned}$$

Taking the limit $N \to \infty$ yields

$$H^h(m,p) = \lambda e^{\beta h} \frac{1-m}{2}(e^{2p}-1) + \lambda e^{-\beta h} \frac{1+m}{2}(e^{-2p}-1),$$

where $p = \phi'(m)$. □

The deterministic macroscopic evolution is recovered through

$$\dot{m} = \partial_p H^h(m, 0),$$

which gives

$$\dot{m} = \lambda e^{\beta h}(1 - m) - \lambda e^{-\beta h}(1 + m).$$

Equivalently,

$$\dot{m}(t) = -2\lambda \cosh(\beta h)\left(m(t) - \tanh(\beta h)\right).$$

Hence the magnetization no longer relaxes towards 0, but towards the shifted equilibrium

$$m_h = \tanh(\beta h).$$

The corresponding Hamilton equations are

$$\begin{aligned}\dot{m} &= \lambda e^{\beta h}(1 - m)e^{2p} - \lambda e^{-\beta h}(1 + m)e^{-2p},\\ \dot{p} &= \lambda \sinh(2p)\cosh(\beta h) - \lambda \cosh(2p)\sinh(\beta h).\end{aligned}$$

As in the symmetric case, the optimal trajectories can be obtained explicitly from these equations. Their qualitative behavior is illustrated in Figure C.1.

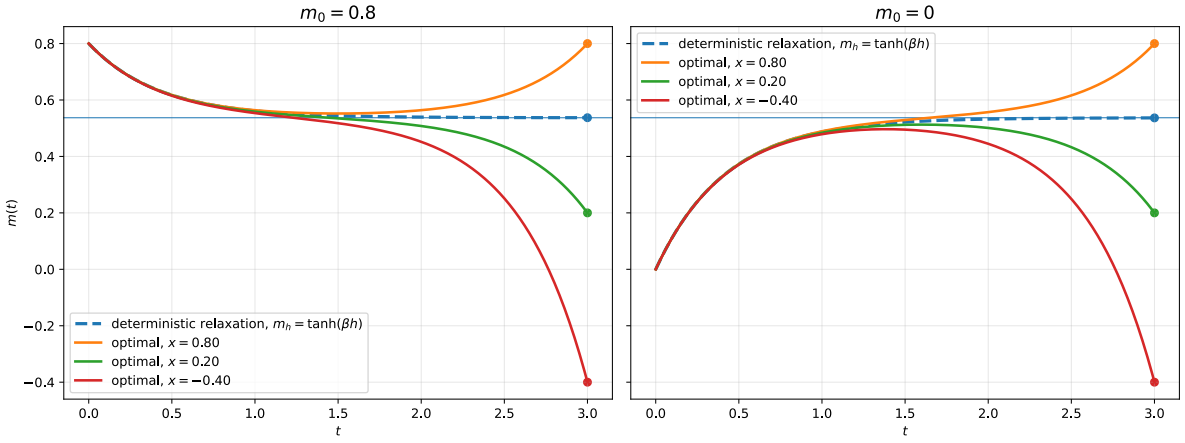

Figure C.1: Optimal trajectories of the magnetization under an external field, for different endpoints x at time $T = 3$, with $\lambda = 1$. The deterministic evolution now relaxes towards the shifted equilibrium magnetization $m_h = \tanh(\beta h)$. Trajectories ending at magnetizations opposed to the field require increasingly large deviations from the deterministic relaxation.

As a consequence of the external field, large fluctuations aligned with the field are naturally facilitated by the dynamics, whereas fluctuations against the field must overcome the deterministic drift towards the preferred equilibrium. The large-deviation structure therefore becomes asymmetric, reflecting how symmetry breaking modifies the geometry of rare fluctuations.

Although the qualitative structure of the optimal trajectories remains close to the symmetric case, the external field provides a simple example in which the macroscopic relaxation is no longer only entropically driven, but also biased by an energetic preference favoring one orientation of the system.